8947

NACA TN 2563

TECH LIBRARY KAFB, NM
0065571

NATIONAL ADVISORY COMMITTEE FOR AERONAUTICS

TECHNICAL NOTE 2563

EXPERIMENTAL INVESTIGATION OF ROLLING PERFORMANCE OF STRAIGHT AND SWEPTBACK FLEXIBLE WINGS WITH VARIOUS AILERONS

By Henry A. Cole, Jr. and Victor M. Ganzer

University of Washington

Washington
December 1951

AFMDC
TECHNICAL LIBRARY
AFL 2811

TECH LIBRARY KAFB, NM
0065571

1T

NATIONAL ADVISORY COMMITTEE FOR AERONAUT...

TECHNICAL NOTE 2563

EXPERIMENTAL INVESTIGATION OF ROLLING PERFORMANCE OF STRAIGHT AND SWEPTBACK FLEXIBLE WINGS WITH VARIOUS AILERONS

By Henry A. Cole, Jr. and Victor M. Ganzer

SUMMARY

Two flexible wings, one with 45° sweepback and the other unswept, were tested by the University of Washington Aeronautical Laboratories to determine their performance in roll. Rolling moments due to aileron deflection, damping derivatives in roll, and free-rolling angular velocities due to aileron deflection were obtained at various speeds including, when possible, the aileron reversal speed.

During the test a secondary flow, which made testing in free roll virtually impossible, was discovered in the test section of the wind tunnel. The condition of free roll was then simulated by driving the model at constant velocity at zero average rolling moment.

The results showed that, when designed for equal stress, the swept wing had generally higher reversal speeds than did the straight wing. Also, it was shown that inboard ailerons for the swept wing were more effective at high speeds than were ailerons extending to the tips.

The experimental values were used to check theory, with good agreement in the case of the straight wing but with unsatisfactory agreement in the case of the swept wing where the theory overestimated reversal speed for all ailerons larger than the 0.2-span ailerons.

INTRODUCTION

The loss in rolling performance at high speeds due to the elasticity of the wing structure of an airplane has been of concern for many years. Until a few years ago airplane wings had little or no sweepback, and the torsional deflection alone was responsible for this loss in rolling performance. This effect usually is identified with the "aileron reversal speed" - the speed at which the ailerons become completely ineffective in rolling the airplane. In recent years large amounts of sweepback

have been incorporated in various airplanes in an attempt to increase critical Mach numbers of the wings. The inclusion of sweepback has made the prediction of rolling performance even more difficult, since the bending deflections of swept wings change the angle-of-attack distribution along the wings. This change, in turn, affects the rolling moments developed as well as the torsional moments about the elastic axis. The inclusion of bending and the greater difficulty in calculating spanwise loadings for swept wings make the theoretical approach difficult and also make the need for experimental data for checking greater.

The experimental data presented in this report consist of the results of tests of two elastic wings, one with sweepback and one unswept. The wings were tested in a fixed position with ailerons deflected, were allowed to roll at equilibrium rolling velocity, and were driven in roll to get damping coefficients.

The tests were conducted in the 8- by 12-foot F. K. Kirsten wind tunnel of the University of Washington Aeronautical Laboratories under the sponsorship and with the financial assistance of the National Advisory Committee for Aeronautics.

SYMBOLS

A	aspect ratio $\left(b^2/S\right)$
b	wing span, feet
c	wing chord, feet
c_n	section normal-force coefficient
c_l	section lift coefficient
C_l	rolling-moment coefficient (L/qSb)
e	distance from wing-section aerodynamic center to elastic axis, fraction of chord
EI	bending stiffness factor
GJ	torsional stiffness factor
L	rolling moment, pound-feet
m_o	section slope of lift curve, per radian

p	rate of roll, radians per second
$pb/2V$	wing-tip helix angle in roll, radians
q	dynamic pressure, pounds per square foot $\left(\frac{1}{2}\rho V^2\right)$
S	wing area, square feet
V	velocity, feet per second
$\frac{y}{b/2}$	nondimensional spanwise station on wing
α	angle of attack, degrees
δ	aileron angle measured in plane parallel to plane of symmetry
Λ	sweepback angle of quarter-chord line, degrees
λ	taper ratio
ρ	mass density of air, slugs per cubic foot
ϕ	angle of roll, degrees or radians

APPARATUS

Wind Tunnel

The F. K. Kirsten wind tunnel, in which the tests were performed, has a filleted rectangular test section 8 by 12 feet. The tunnel is of the double-return type, driven to a maximum velocity of 250 miles per hour by two 750-horsepower direct-current motors connected to $14\frac{3}{4}$-foot-diameter, seven-bladed fans mounted in each return duct. The tunnel has a contraction ratio of 6.3, and the expansion is effectively a $7\frac{1}{3}^{\circ}$ angle. The rearward end of the test section is vented to atmospheric pressure through a slot. A drawing of the wind tunnel may be found in figure 1, and a more detailed description is presented in reference 1.

Model Mount

The model mount consisted of a shaft carried in ball bearings within a housing, which was attached to the standard model-mounting-support system

(see figs. 2 and 3). A torsion spring with four strain gages installed to read torsional loads only was placed between the forward bearing and the wing. Leads from the strain gages were brought through a four-conductor plug when the wing was held in position and through silver slip rings with double carbon brushes when the wing was rotating. The voltage output of the strain-gage bridge was balanced by an SR-4 type K strain indicator. A cathode-ray oscillograph was used to indicate rapid variation of rolling moment in order that a good average might be obtained.

During the test it was found that the torsional spring did not offer enough stiffness in bending, and flutter resulted at speeds well below the desired test speeds. This condition was improved by extending a beam from the part of the sting in front of the torsional spring to a point well behind the spring and by mounting this beam in flexures to take the bending loads without introducing an appreciable amount of torsional stiffness.

The only method of measuring rolling velocity was by means of 10 contact points mounted at equal distances around the shaft. The impulses from these contacts were recorded on a clock-driven tape.

The model was driven in roll by means of a 3/4-horsepower, direct-current, 24-volt electric motor which was connected to the rearward end of the rotating shaft through a gear train. Both the impressed voltage and the field current were variable for speed control.

Models

Two model wings were constructed with structure sufficiently flexible to allow reversal speeds to fall within the capabilities of the wind tunnel. Some of the characteristics of the wings are listed in table I, and aileron combinations are illustrated in figure 4.

The wings were constructed of balsa segments fastened to beryllium copper spars as shown in figures 5 to 8. The spars were located at the 38-percent-chord line - a reasonable value of the elastic axis of modern wings. Thin rubber was glued over the slots between the balsa segments.

The ailerons were attached to brackets which in turn were fastened directly to the wing spar. Care was taken in the design so that the stiffness of the ailerons, which were of solid balsa, could not add to the stiffness of the wing structure. The ailerons were sealed by rubber strips on the pressure side. Photographs of the completed wings are shown in figures 3 and 9.

Figure 10 shows the EI and GJ curves from which the model spars were designed. It will be noted that these curves are cubic in nature, a

variation of EI and GJ with span which was found to be representative of modern airplanes. The philosophy used in designing the spars was that the same maximum stresses should occur in the spars with the same spanwise loading distribution. For a sweepback of 45°, the bending moment in the spar is $2^{1/2}$ times the moment in a straight-wing spar for the same loading, giving spar dimensions for the swept wing $2^{1/6}$ times those for the straight-wing spar.

In constructing the spars, which were ground to tolerances of 0 to 0.001 inch, the tendency was to make them slightly oversized; thus the EI and GJ values for the final wings were somewhat greater than the original design values. Also, the addition of the rubber seal strips increased the wing bending stiffness by 0.7 percent in bending and 0.9 percent in torsion. For these reasons, the actual deflections of the wings for a given load were slightly less than the deflections computed from the design EI and GJ curves.

Deflections of the final wings due to a 1-pound load applied at $\frac{y}{b/2} = 0.966$ for bending and a 1-pound-inch torque applied at $\frac{y}{b/2} = 1$ are listed in table II.

The values in table II, with computed values from the design EI and GJ curves, using the method of reference 2, are plotted in figures 11 and 12. In making theoretical calculations regarding the rolling performance of the wings, the EI and GJ curves were adjusted to fit the experimental values.

Another wing model was constructed in the form of a cross, as shown in figures 13 and 14. This model was built of solid mahogany and had a span of 4 feet, a constant chord of 6 inches, and a symmetrical wing section. It was not built to usual model standards but was built quickly and simply to test qualitatively the effect of the added wing panels on the instantaneous rolling velocity in free roll.

PROCEDURE

The preliminary plans for the test called for measurement of rolling moment at various velocities with various ailerons and with the models held fixed, measurement of damping derivatives at various speeds with the models driven by the motor, and measurement of the equilibrium rolling velocities at various speeds and with various ailerons deflected.

The first free-rolling tests showed a tendency of the model to stop rolling at a certain position in the tunnel at speeds well below the reversal speed. This led to a check of the instantaneous rolling velocity, as obtained from the electrical contacts, with the results plotted in figure 15. These results showed that the rolling velocity was a function of the position of the model in the tunnel at all speeds and that any attempt to measure $pb/2V$ by free roll would be futile.

It was found that similar results had been obtained previously in three different wind tunnels of rectangular cross section, both open- and closed-return types (reference 3). This would indicate that the type of flow causing this phenomenon might be inherent in this type of tunnel. Results from circular-cross-section tunnels were not found.

Reference 3 indicates that a secondary flow, which consists of a component of the main flow toward the corners, is present in tunnels of rectangular cross section. The existence of such a flow was checked in the University of Washington wind tunnel by means of a standard yaw-and-pitch-head survey in the test section. The results of this test, found in figure 16, show definitely that such a secondary-flow pattern exists with velocities in a plane normal to the tunnel center line.

Various devices were installed in the wind tunnel in an attempt to affect this secondary flow. These included a duct around the permanent model-support strut in an attempt to localize its effects, screens just ahead of the contraction, and various spoilers to change the relative quantity of flow through each return passage. None of these attempts resulted in any appreciable improvement in the flow characteristics.

After spending some time on the investigation of the wind tunnel it was decided that any attempt to make the flow in the wind tunnel satisfactory for the type of test contemplated, even if possible, would result in a major investigation and would require a large amount of time and money. Hence, techniques of testing which might use the wind tunnel with its obvious shortcomings were considered. These techniques were:

(1) Use of flow straighteners: It was thought that a circular tube - essentially a tunnel within a tunnel - with honeycomb, screens, or whatever was necessary, might be placed around the wing. This was discarded because of the development time necessary, again with no assurance that the method would succeed.

(2) Use of a correction factor: In reference 3 a method of applying a correction factor to the average rolling velocity was developed. However, in reference 3 only rigid wings were used; hence, an average rolling velocity was always available. In the present test of the flexible wing, the secondary flow caused the wing to stop rolling altogether at

speeds below the true reversal speed. Therefore, no conceivable correction factor could be derived which could be applied to a velocity of zero to give the true rolling velocity.

(3) Use of a large moment of inertia: It was proposed that a device such as a flywheel be mounted on the shaft to force the wing to roll at essentially a constant velocity. This method, although promising, was discarded in favor of method (4).

(4) Use of motor to drive model: In this method, which was the one adopted, the motor was used to drive the model at essentially constant rolling velocity; this velocity was adjusted to make the average rolling moments zero as determined by the strain-gage readings. It was assumed that the rolling velocity thus obtained approximated the free-rolling velocity which would have been obtained by a wing rolling in a perfect-air jet. This method, as the rolling velocity approached a constant, gave an effective moment of inertia approaching infinity. It had another advantage in that bearing friction in the shaft was not a factor in the rolling velocity developed by the wing, since the strain gages were mounted ahead of the bearings.

(5) Use of crossed wings: The evidence of the secondary flow in the wind tunnel may be obtained by measuring the rolling moment of a wing held at various angles of roll. Any component of the main flow perpendicular to the wing will result in a rolling moment. This was done with the flexible straight wing, with the results shown in figure 17. These results indicated that the impressed rolling moment due to the secondary flow was almost symmetrical. It was reasoned that a pair of wings mounted perpendicular to each other would roll at constant velocity, if the impressed rolling moment was symmetrical. Thus, if no drive motor was available, such a wing system might give acceptable results. However, it must be realized that the model-building problem is complicated by this technique. A simple wing system, shown in figures 13 and 14, was constructed to test this theory. The possibility of using two counterbalanced wing panels mounted at 90° is indicated also, but this was not tried.

It should be mentioned that the reliability of the results of all of these methods depends upon the premise that the average condition, as interpreted, gives the correct answer. It has already been shown that this is not true if the average rolling velocity of a free-rolling model is considered; hence, the validity of the assumption depends on the technique used. If all variations were linear, it would seem logical that the technique used in this test would give good results.

The actual tests consisted of the following:

(1) C_l against q (figs. 18 and 19): The wings were held horizontally in the wind tunnel, and rolling-moment coefficients were obtained with various ailerons deflected. The aileron reversal speed was obtained by plotting C_l against q, the value of q where $C_l = 0$ being the q for reversal. The results shown are averages of aileron deflections for plus and minus rolling moment.

(2) C_l against $pb/2V$ (figs. 20 and 21): The wings were driven with ailerons undeflected by the electric motor at various values of p. The rolling moments measured, called the damping moments in roll, are plotted against the wing-tip helix angle $pb/2V$. Averages of right and left roll are presented in the figures.

(3) $\frac{\partial C_l}{\partial\left(\frac{pb}{2V}\right)}$ against q (fig. 22): The damping derivative $\frac{\partial C_l}{\partial\left(\frac{pb}{2V}\right)}$ was obtained by measurement of the slopes of the curves of C_l against $\frac{pb}{2V}$ at $\frac{pb}{2V} = 0$. The slopes are plotted for both wings in the figure indicated.

(4) $\frac{pb}{2V}$ against q (figs. 23 to 25): With various ailerons deflected, the wings were driven at rolling velocities such that the average rolling moment was zero. Plots of $\frac{pb}{2V}$ against q were made from the data obtained. Again the data presented are the averages obtained from aileron deflections for plus and minus rolling velocities. Where possible, data from free-roll tests are presented also. For very high rates of roll, only values for free roll are presented since motor limitations would not permit rolling the model with the motor.

(5) p against ϕ for rigid wings (fig. 26): A single rigid wing with ailerons deflected was allowed to roll freely, and the resulting instantaneous rolling velocity p was plotted against ϕ, the angle of the wing in the tunnel. A second wing, similar geometrically, was fastened perpendicular to the first, as shown in figure 14. This combination was allowed to roll freely, giving another set of data for the plot. Note again that the data were obtained from the contacts on the sting and represent average conditions over a small portion of a complete revolution. However, the qualitative value of the results is not impaired because of this lack of precision.

It is evident, for many aileron configurations, that data were not obtained at high enough velocities to approach aileron reversal speeds. This lack of data was the result, principally, of consideration for the models. In some of the tests a tendency to flutter was noticed at high speeds, and for other tests the deflections became alarmingly great. Hence, tests were stopped at speeds deemed safe with regard to preservation of the models.

No wind-tunnel-wall corrections were applied to the data presented. The wings were small compared with the tunnel, and for many of the tests the lift on the model was very small, which should make the corrections small.

DISCUSSION

Comparison of straight and swept wings.- A comparison of the results obtained from tests of the straight and swept wings may be made with regard to the rolling moment developed, the damping moments, and the helix angle in roll.

The rolling-moment coefficients of the swept wing reduced much more rapidly with q than did those of the straight wing (see figs. 18 and 19). This may be explained by the fact that the bending of the swept wing due to the load produced by the ailerons caused an additional change in the effective angle of attack near the tips, tending to counteract the effect of the ailerons. This effect, which is inherent because of the geometry of swept wings, does not occur with straight wings, for which bending produces no change in the effective angle of attack.

Aileron reversal speeds, which may be obtained by extrapolating to the value of q at which $C_l = 0$, were quite definite for the straight wing, since the curves of C_l against q crossed the axis with a fairly large slope. Also, the aileron reversal speeds were nearly alike for all of the conventional aileron spans, being about 136 miles per hour for the 0.2-span ailerons and about 140 miles per hour for the 0.4-span ailerons.

For the swept wings the aileron reversal speeds were not so definite, since the curves of C_l against q crossed the axis with a slope approximately equal to 0. Hence, a very small error in measuring rolling moment could change the reversal-speed estimation by a large amount, particularly if the curves had to be extrapolated, as was necessary in this test. An approximate extrapolation of the data presented in figure 19 indicates that the aileron reversal speeds varied widely with ailerons of different span for the swept wing. However, the only definite reversal speed obtainable was 125 miles per hour for the 0.2-span aileron.

It is doubtful whether the aileron reversal speed is a good criterion for swept-wing aileron design. The initial rolling moment developed upon deflection of the aileron is very important, in that this moment must accelerate the airplane in roll. Figure 19 shows that airplanes with swept wings and conventional ailerons may have high initial rolling moments at very low speeds and high reversal speed but may have relatively low initial rolling moments at speeds well below reversal speed. An investigation into the dynamic behavior of an aircraft with flexible swept wings, upon deflection of the ailerons, might be a more satisfactory method for determining the merit of a particular aileron.

Damping-moment derivatives were obtained from plots of C_l against $pb/2V$ as in figures 20 and 21. At low values of q, these curves were linear, but at larger values of q they tended to become nonlinear for the straight wing because of the large amount of twist and, thus, possible stall at the tip. The bending of the swept wing alleviated this tendency. The slopes of the curves were measured at $pb/2V = 0$ in order to obtain the damping derivatives $\frac{\partial C_l}{\partial\left(\frac{pb}{2V}\right)}$.

The values of the damping derivatives are plotted for both wings in figure 22. As was expected, the straight-wing damping derivatives increased in value with q, because of the fact that the aerodynamic center of the wing section was approximately 13 percent of the chord ahead of the torsional axis, giving positive twist with positive angle of attack. On the other hand, the swept-wing values decreased, since the reduction of the derivative due to wing bending more than offset the increase due to twist.

The results of the tests with ailerons deflected and the models rolling at zero average rolling moment, shown in figures 23 and 25, confirmed that the aileron reversal speeds were almost the same for all percent-span ailerons for the straight wing and were different for the swept wing. It would appear advantageous to use a large-span aileron on a swept wing if reversal speed were the design criterion. The aileron reversal speeds obtained from the curves of $pb/2V$ against q checked very closely with those obtained from the rolling-moment-coefficient data already discussed. This substantiates the validity of the method of rolling the model at the zero average moment and using the results as though the model were rolling in free air.

Comparison of inboard and outboard ailerons.- Figure 25 shows data obtained with the swept-wing ailerons not extending to the tip. The data showed that a 0.2-span aileron extending from $\frac{y}{b/2} = 0.6$ to 0.8 produced about half as much rolling velocity at low speed as did a 0.4-span aileron

extending from $\frac{y}{b/2} = 0.6$ to the tip; but at $q = 40$ the rolling velocity was identical for each aileron, while at values of q above 40 the smaller aileron was superior. This was true also for a 0.4-span aileron from $\frac{y}{b/2} = 0.4$ to 0.8 as compared with a 0.6-span aileron from $\frac{y}{b/2} = 0.4$ to the tip, with $q = 40$ again the value at which the smaller aileron became superior. The same superior performance for the wing with inboard ailerons was evident from the rolling-moment coefficients as plotted in figure 19.

Comparison of results with theory.- Theoretical values were available from several sources for most of the items found experimentally in this test, notably the values of C_l, $\frac{\partial C_l}{\partial\left(\frac{pb}{2V}\right)}$, and $pb/2V$ at $q = 0$ (rigid-wing values), the variation of these values with q from at least one source, and the reversal speeds. The values obtained from these sources will be discussed briefly.

(1) Rolling-moment coefficient C_l per degree aileron deflection: Two theoretical methods were used to get the rolling-moment coefficients for the straight wing at $q = 0$, which corresponds to a wing with infinite stiffness. From reference 4 values of C_l were obtained by interpolating for values of the rolling-moment factor F_2 from table VII. The following values resulted, using $m_o = 5.66$ and $\left(\frac{\partial\alpha}{\partial\delta}\right)_{c_n} = -0.64$:

Aileron (percent span)	F_2	$\frac{C_l}{\partial\delta}$ at $q = 0$
20	0.0136	0.00229
40	.0282	.00475
60	.0422	.00712
80	.0512	.00863
95	.056	.0094

Reference 2, a thesis written at the University of Washington, gives values of C_l for values of q other than 0, as well as for $q = 0$. The thesis should give values quite close to those obtained in reference 4 at $q = 0$, since it is similar in approach. An assumption was made that the spanwise variation c_l for $\lambda = 0.5$, as obtained from

reference 4, was the same as that for $\lambda = 0.45$, the actual value for the wing. This would affect the accuracy somewhat. The results from this theoretical approach are tabulated below.

Aileron (percent span)	$C_l/^{\circ}\delta$ at -			
	q = 0	q = 27.7	q = 41.5	q = 55.4
20	0.00214	0.00135	0.00062	-0.00083
40	.00487	.00313	.00144	-.00184
60	.00725	.00473	.00237	-.00232
80	.00908	-------	-------	--------

The above results are plotted, along with the experimental data, in figure 18 and check quite closely.

For the swept wing, theoretical values were obtained using reference 2, with $m_o = 5.66$ and $\left(\frac{\partial\alpha}{\partial\delta}\right)_{c_n} = -0.64$.

Aileron (percent span)	$C_l/^{\circ}\delta$ at -				
	q = 0	q = 23.64	q = 40	q = 47.28	q = 70.92
20	0.00136	0.000177	0.00001	-0.000035	-0.000098
40	.00342	.000925	.00051	.00037	.000105
60	.00538	.0019	.00124	.00104	.00058

The above values are plotted in figure 19. The theoretical values checked the experimental values for the 0.2-span aileron quite closely but were too high for the 0.4- and 0.6-span ailerons. This lack of confirmation could have been due to lack of agreement between actual and theoretical lift distribution, particularly near the tip, which is critical. It also may have been due to the use of an erroneous moment coefficient due to aileron deflection or to an error in the assumed spanwise variation of moment coefficient. It would appear that these factors should receive more attention if the theory is to check experimental data.

Also, since small errors in computing C_l at high values of q could result in large changes in reversal speed because of the low slope of the curves as they pass through $C_l = 0$, the precision of the theoretical method might be at fault. All of the computations were accomplished by the use of five-by-five matrices, and it is possible that ten-by-ten matrices, for example, might give better results.

(2) Damping derivatives in roll: By reference 4, using $m_o = 5.66$ and $F_5 = 0.032$, the damping derivative at $q = 0$ for the straight wing was $\frac{\partial C_l}{\partial\left(\frac{pb}{2V}\right)} = -0.48$.

From reference 2, using the lift distribution from reference 4 instead of the one shown in the example in reference 2, and e (the distance from the a.c. to the elastic axis) = 0.13 and 0.14, the damping derivatives became

$q_{e=0.14}$	$q_{e=0.13}$	$\frac{\partial C_l}{\partial\left(\frac{pb}{2V}\right)}$
0	0	-0.48
25.7	27.7	-.703
38.5	41.5	-.933
51.5	55.4	-1.445

The above values were plotted in figure 22. Fair agreement existed at low values of q, but at higher speeds the experimental tests gave higher damping derivatives than the theory. This may have been due to the drag component, which would tend to increase the wing twist when the tip was deflected. This component was neglected in the theory.

It also is possible to obtain $\frac{\partial C_l}{\partial\left(\frac{pb}{2V}\right)}$ by dividing the experimental values of C_l from figure 18 by the values of $pb/2V$ from figure 23. Damping derivatives obtained in this way check the theoretical values for the straight wing with $e = 0.13$ very closely. Since the tip deflections were less for the tests shown in figures 18 and 23 than for the tests in which the wing was driven in roll, and since the drag component would be of less importance with the smaller tip deflections, the possibility exists that the drag component caused the discrepancy between theory and experiment.

It should be noted that the damping derivative is quite sensitive to e, which is hard to estimate on such a small model.

For the swept wing, reference 5 was used to get the damping derivative at $q = 0$, resulting in the value of $\frac{\partial C_l}{\partial\left(\frac{pb}{2V}\right)} = -0.37$. This value should be compared with the experimental value of about -0.42.

Reference 2 was used also and, for $e = 0.13$, gave

$q_{e=0.13}$	$\frac{\partial C_l}{\partial\left(\frac{pb}{2V}\right)}$
0	-0.433
23.64	-.192
40	-.146
47.28	-.12
70.92	-.089

The above values, which are plotted in figure 22, agree quite closely with experimental data.

It might be noted that the damping derivatives of highly swept wings are not so sensitive to the value of e as are those of straight wings. Also, since tip deflections are not so large as those for straight wings, the drag component is not so important. These facts may account for the better agreement between theory and experiment with the swept wing than with the straight wing.

(3) Rolling velocity due to ailerons: The rolling velocities due to ailerons, as indicated by $pb/2V$, were obtained for the straight wing at $q = 0$ by the use of reference 4, resulting in the following values:

Aileron (percent span)	$\frac{pb/2V}{\alpha_\delta}$ at $q = 0$
20	0.0047
40	.0098
60	.0147
80	.0178
95	.0195

Using reference 2, the following values were obtained for $e = 0.13$:

Aileron (percent span)	$\frac{pb/2V}{\sigma_\delta}$ at -			
	$q = 0$	$q = 27.7$	$q = 41.5$	$q = 55.4$
20	0.00446	0.00192	0.000662	-0.00061
40	.01015	.00445	.00154	-.00135
60	.0151	.00673	.00253	-.00171

Using reference 6, a value of q at reversal was found. In this case $m_o = 5.66$ and a value of $C_{p_\delta} = 0.471$ obtained by using a lift-curve slope corrected for induced effects were used. For the 0.3 chord and 40-percent-span ailerons, a value of q at reversal of 66 pounds per square foot resulted. If a section value of C_{p_δ} had been used, a considerably higher reversal speed would have resulted.

Other reversal speeds were calculated from references 7 and 8.

All of the above data were plotted in figures 23 and 24. Agreement with experiment was fair, although the value of q for reversal obtained from reference 6 was very high. Reference 2 gave the best agreement of all for the straight wing.

For the swept wing, using the experimental stiffness values and $C_{p_\delta} = 0.448$, reference 6 gave a value of q at reversal of 75 pounds per square foot for the 40-percent-span ailerons.

Reference 2 gave the following values:

Aileron (percent span)	$\frac{pb/2V}{\sigma_\delta}$ at -	
	$q = 0$	$q = 40$
20	0.00314	0.00007
40	.0079	.0035
60	.0124	.0085

The above values, which were plotted in figure 25, showed good agreement at low speed but overestimated reversal speed for all except the tip ailerons. In the case of the method of reference 2, this was due mainly to the overestimation of rolling-moment coefficients at high speed, and the comments made concerning those coefficients apply here also.

Four-panel-wing system.- Figure 26 shows that the addition of a perpendicular wing, making a four-panel wing in the form of a cross, reduced the variation of rolling velocity with position in the tunnel almost to 0. This probably would work only when the impressed rolling moment due to the secondary flow was symmetrical. However, in this case, the method might hold some promise. It is interesting to note that the steady rolling velocity obtained from the four panels was higher than the average rolling velocity obtained from two panels.

SUMMARY OF RESULTS

The following results were obtained from an investigation to determine the performance in roll of two flexible wings, one swept back 45° and the other unswept:

1. When designed for equal stress, aileron reversal speeds were higher for a swept wing than for a straight wing for all ailerons except short tip ailerons.

2. Aileron reversal speeds for a straight wing occurred at nearly the same speed with all percent-span ailerons but varied widely for a swept wing.

3. Ailerons mounted inboard on a swept wing resulted in much higher reversal speeds than did the same percent-span ailerons mounted at the tips.

4. Theoretical values obtainable for straight wings checked experimental values quite closely. The agreement was not satisfactory for the swept wing, with the theory overestimating the reversal speeds in most cases.

University of Washington
Seattle, Wash., March 28, 1951

REFERENCES

1. Kirsten, Frederick K., and Eastman, Fred S.: The University of Washington's New 250 m.p.h. 8 × 12 Foot Wind Tunnel. Jour. Aero. Sci., vol. 6, no. 12, Oct. 1939, pp. 494-498.

2. Cole, Henry Ambrose, Jr.: Determination of Rolling Characteristics of Flexible Wings with Sweepback by Matrix Methods. M. S. Thesis, Univ. of Wash., June 1950.

3. Evans, J. M., and Fink, P. T.: Stability Derivatives - Determination of l_p by Free Rolling. Rep. ACA-35, Australian Council for Aeronautics, May 1947.

4. Pearson, H. A.: Theoretical Span Loading and Moments of Tapered Wings Produced by Aileron Deflection. NACA TN 589, 1937.

5. Polhamus, Edward C.: A Simple Method of Estimating the Subsonic Lift and Damping in Roll of Sweptback Wings. NACA TN 1862, 1949.

6. Diederich, Franklin W.: Calculation of the Effects of Structural Flexibility on Lateral Control of Wings of Arbitrary Plan Form and Stiffness. NACA RM L8H24a, 1948.

7. Shornick, Louis H.: The Computation of the Critical Speeds of Aileron Reversal, Wing Torsional Divergence and Wing-Aileron Divergence. MR No. ENG-M-51/VF18, Addendum 1, Materiel Center, Army Air Forces, Dec. 19, 1942.

8. Pearson, Henry A., and Aiken, William S., Jr.: Charts for the Determination of Wing Torsional Stiffness Required for Specified Rolling Characteristics or Aileron Reversal Speed. NACA ACR L4L13, 1944.

TABLE I

WING CHARACTERISTICS

	Straight wing	Swept wing
Wing area, S, sq ft	2	2
Wing span, b, ft	4	4
Taper ratio, λ	0.45	0.45
Sweepback angle, Λ, deg	0	45
Aspect ratio, A	8	8
Airfoil section	NACA 63A012	NACA 63A012
Twist	0	0
$\frac{\text{Aileron chord}}{\text{Wing chord}}$	0.3	0.3
$\frac{\text{Aileron span}}{\text{Wing span}}$	0.2, 0.4, 0.6, 0.8, [a]0.95	0.2, 0.4, 0.6, 0.8, [a]0.95, [b]0.2 inboard, [b]0.4 inboard

[a]The ailerons denoted as covering 0.95 of the span abutted the housing over the central attachment fittings and hence were effectively full-span ailerons.

[b]The 0.2 inboard ailerons extended from $\frac{y}{b/2} = 0.6$ to 0.8, and the 0.4 inboard ailerons extended from $\frac{y}{b/2} = 0.4$ to 0.8.

TABLE II

DEFLECTIONS OF WINGS DUE TO LOAD

[1-lb load applied at $\frac{y}{b/2} = 0.966$ for bending;

1-lb-in. torque applied at $\frac{y}{b/2} = 1$]

$\frac{y}{b/2}$	Straight wing		Swept wing	
	Bending deflection (in.)	Twist (deg)	Bending deflection (in.)	Twist (deg)
0.259	0.043	0.073	0.064	-----
.5	.240	.270	.435	0.252
.707	.589	.751	1.089	.615
.866	.981	1.309	1.893	1.148
.966	1.379	-----	2.484	-----
1.00	-----	2.24	-----	1.85

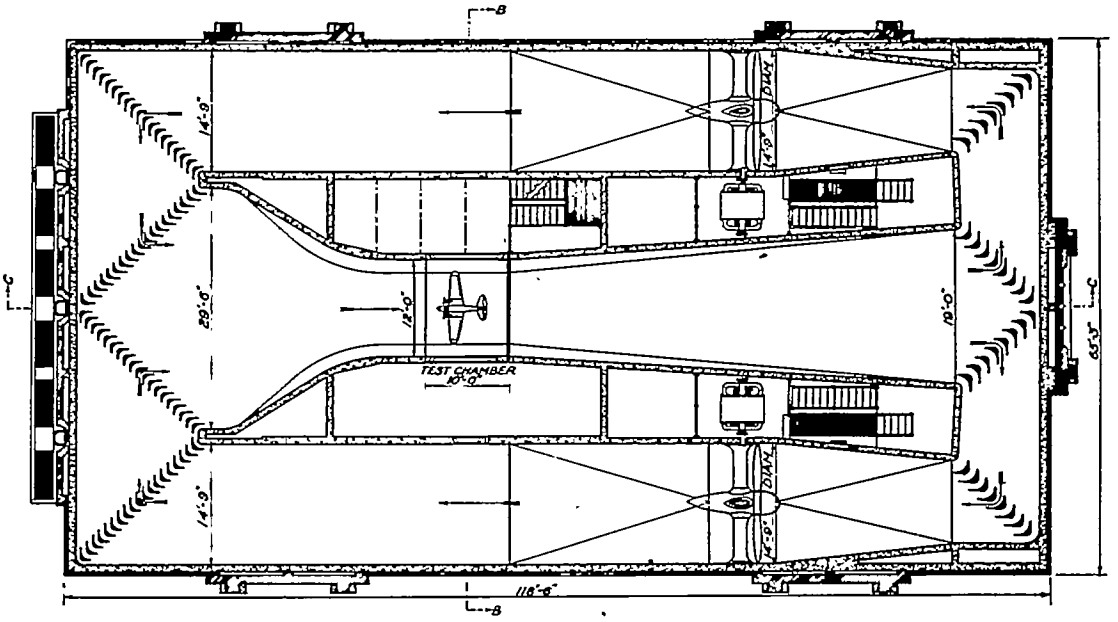

SECTIONAL PLAN THROUGH TUNNEL AXIS

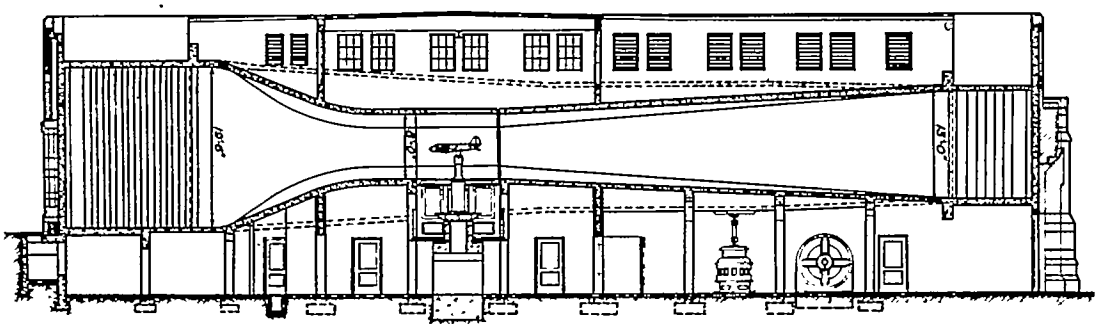

SECTIONAL ELEVATION "C"

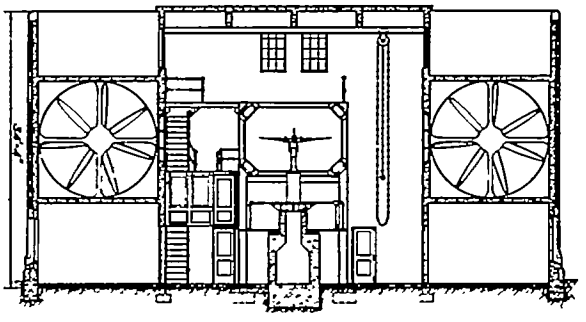

SECTIONAL ELEVATION "B"

Figure 1.- University of Washington 250 mph wind tunnel.

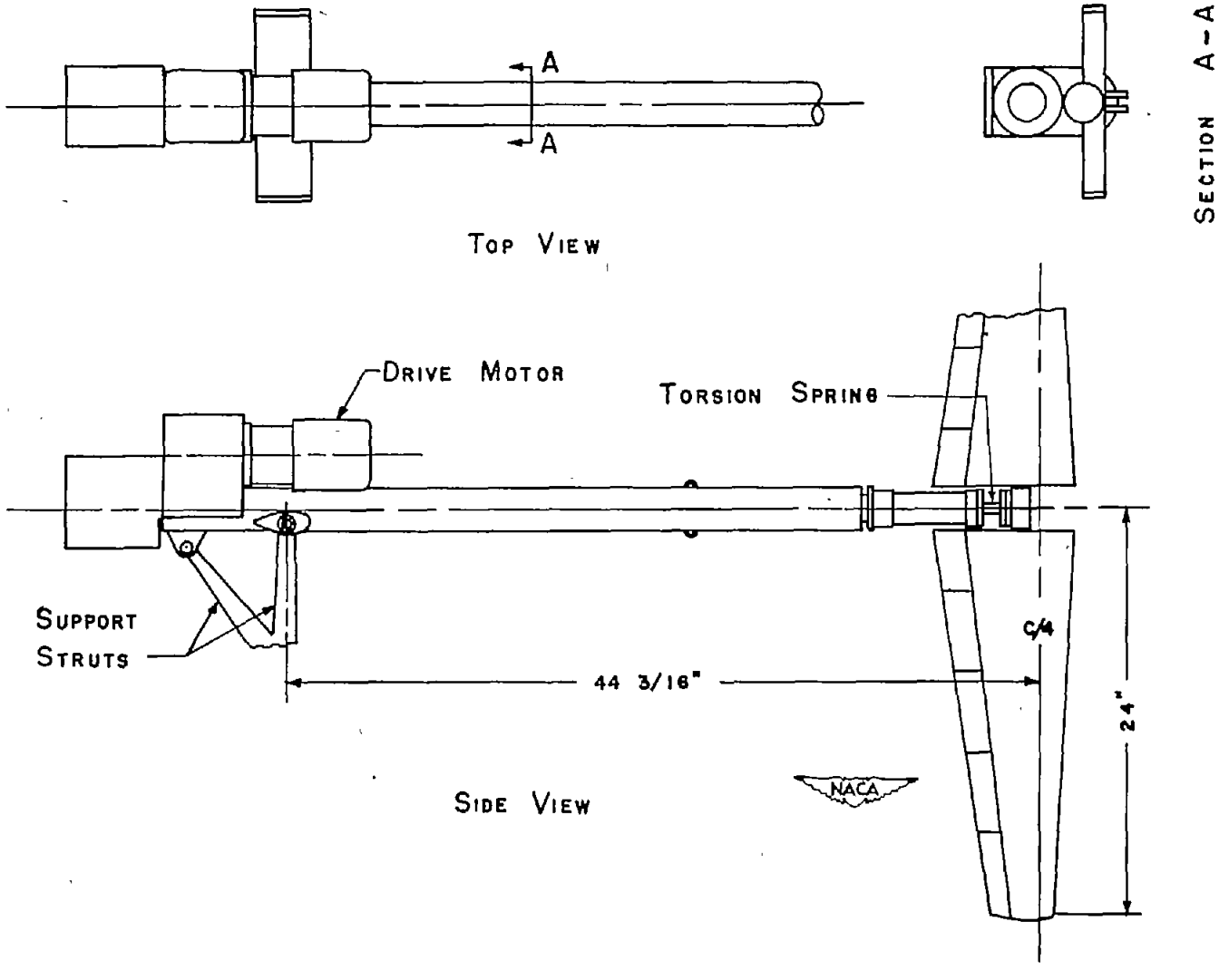

Figure 2.- Model mount.

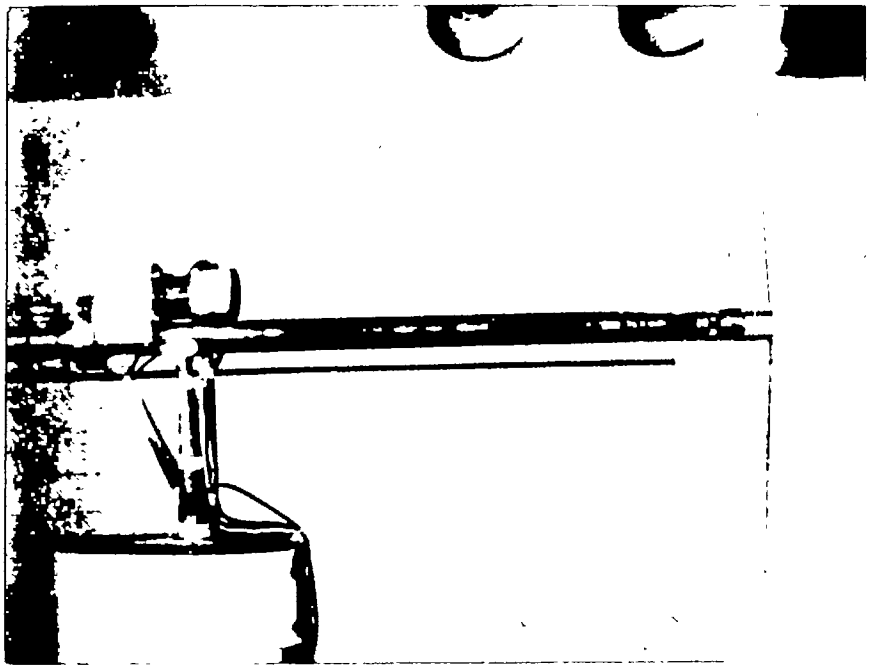

(a) Side view.

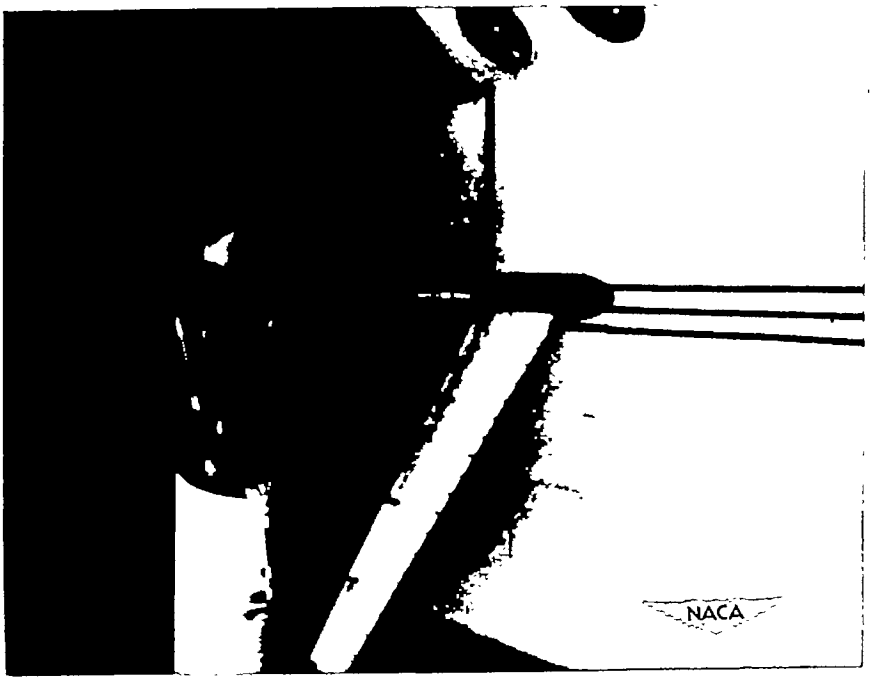

(b) Three-quarter front view.

Figure 3.- Photograph of model mount and straight wing.

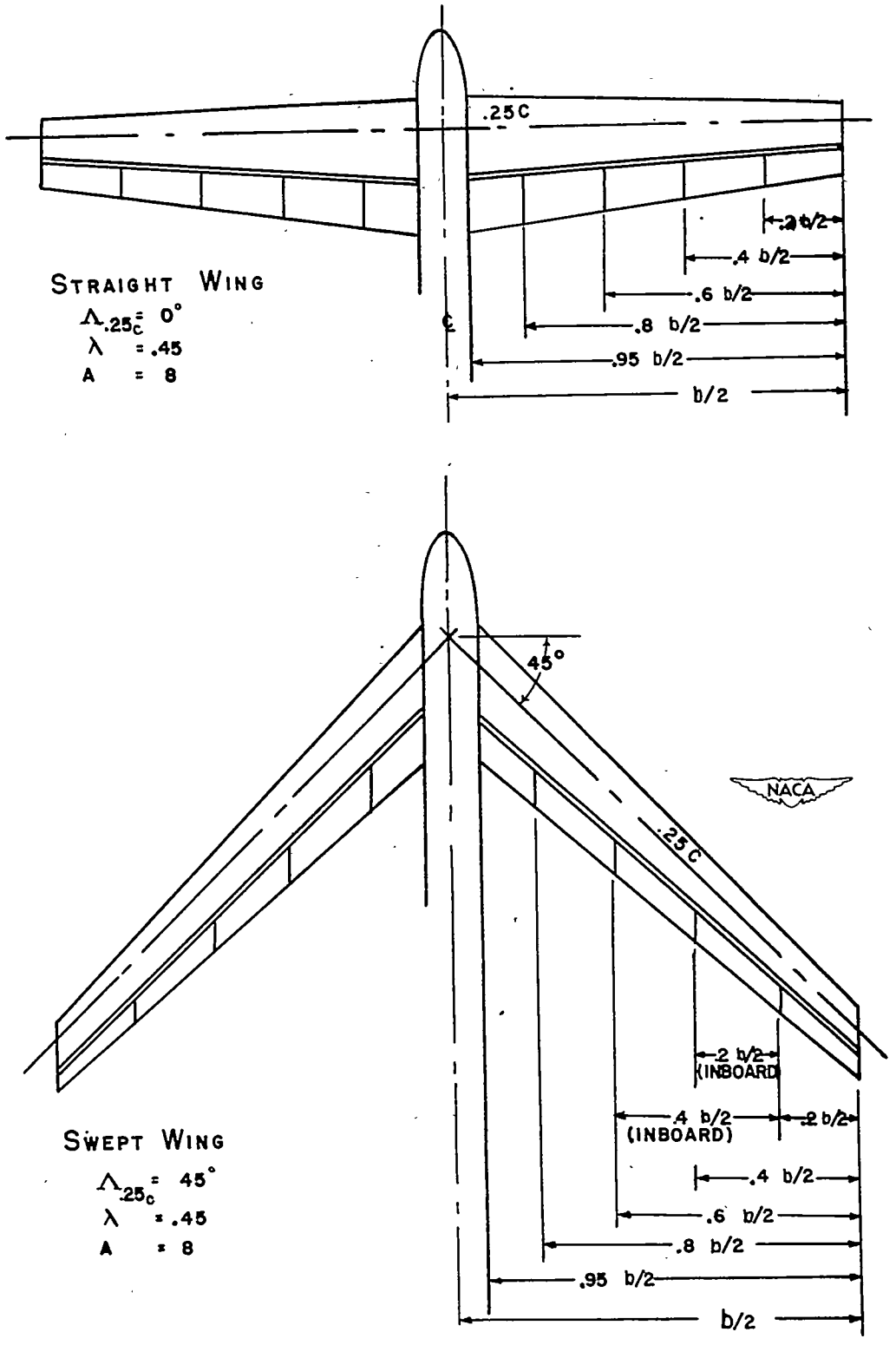

Figure 4.- Aileron combinations.

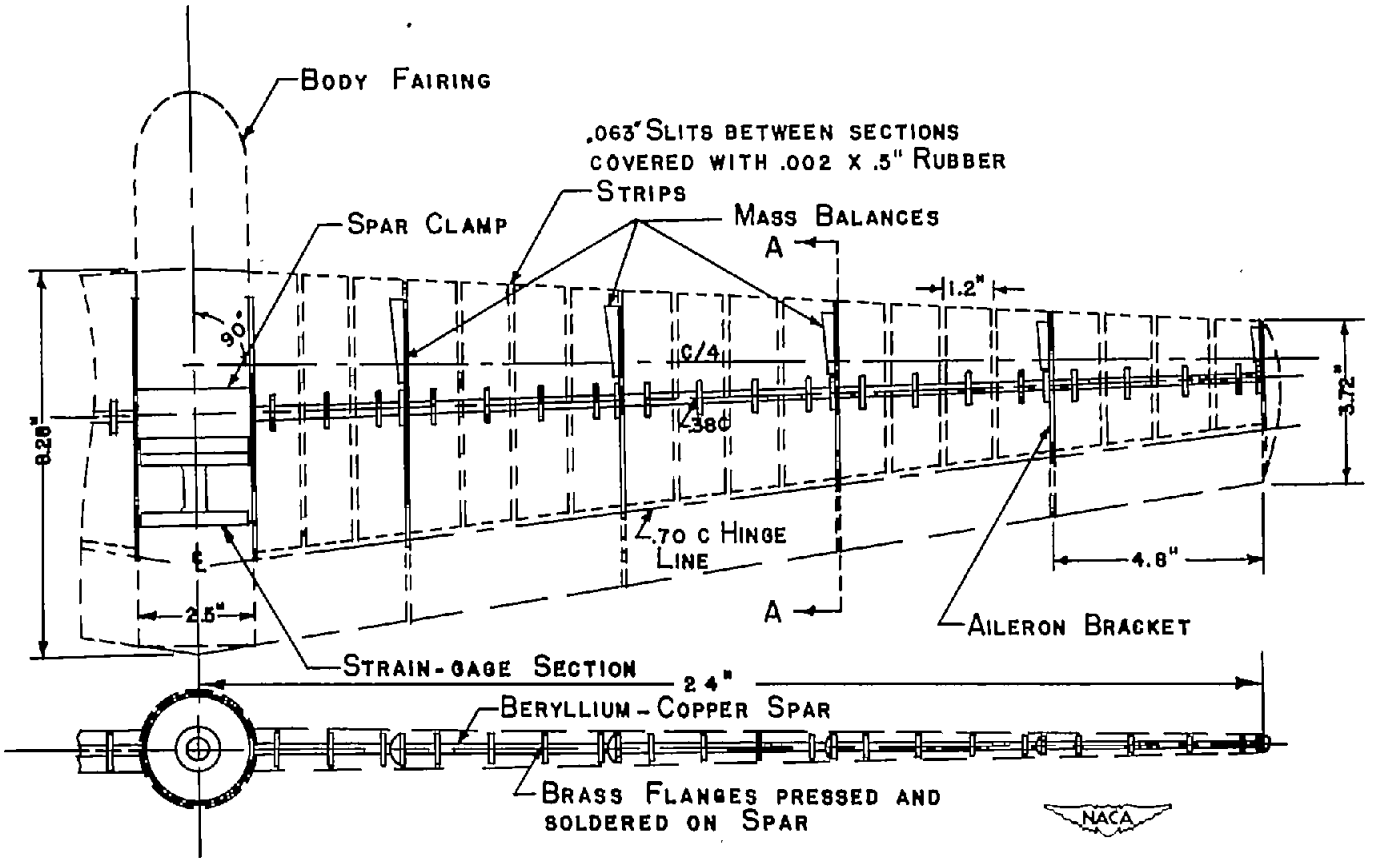

Note: Solid lines show structural metal parts. Broken lines show airfoil outlines which are balsa-wood parts.

See Fig.6 for detail of Section A-A

Figure 5.- Flexible wing.

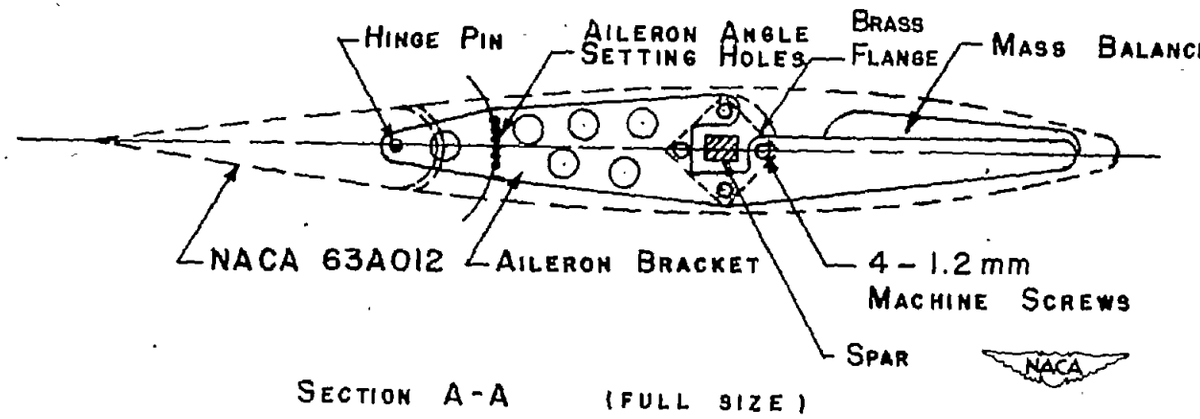

Figure 6.- Flexible-wing-section detail.

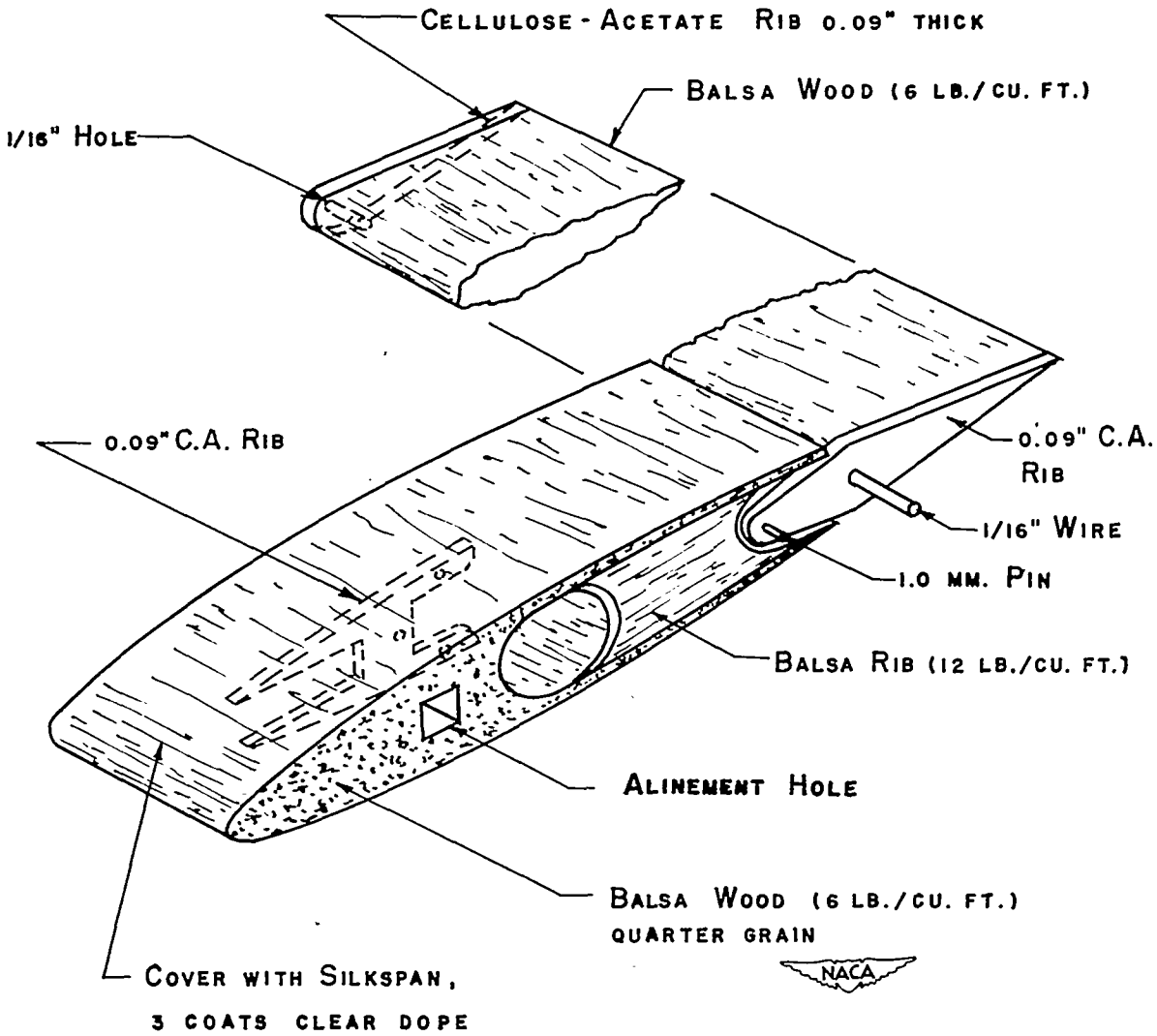

Figure 7.- Wing-section detail.

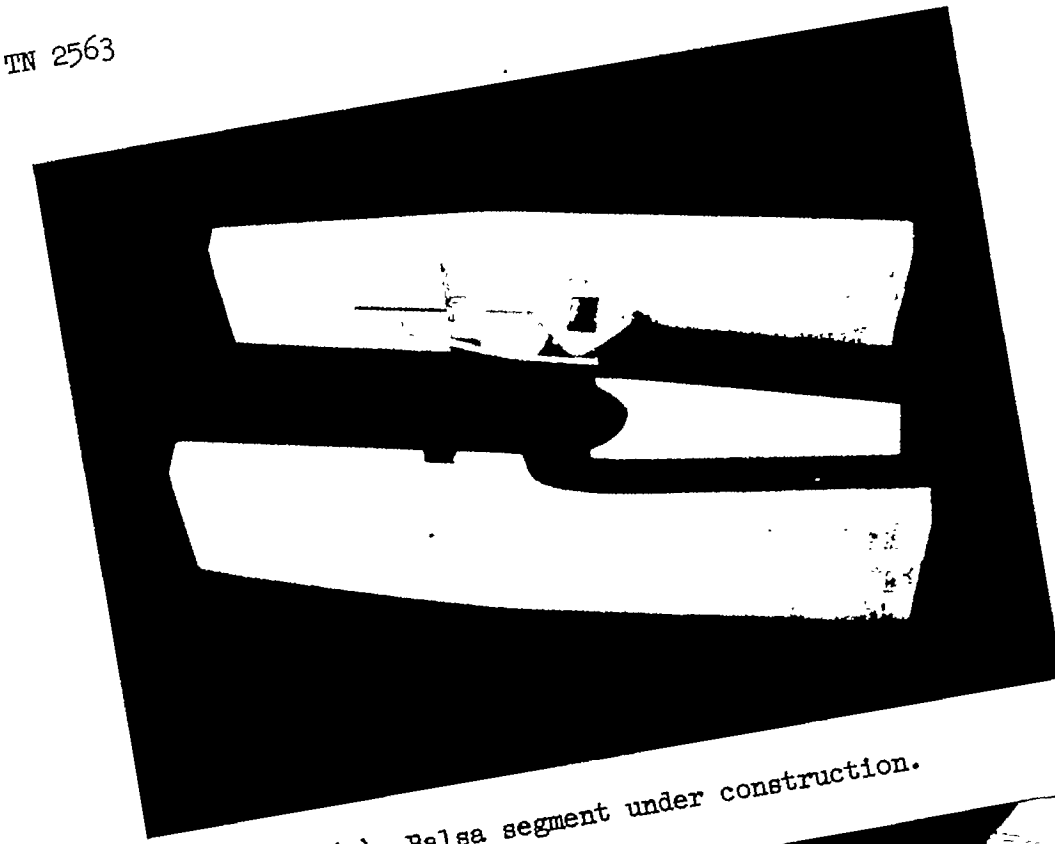

(a) Balsa segment under construction.

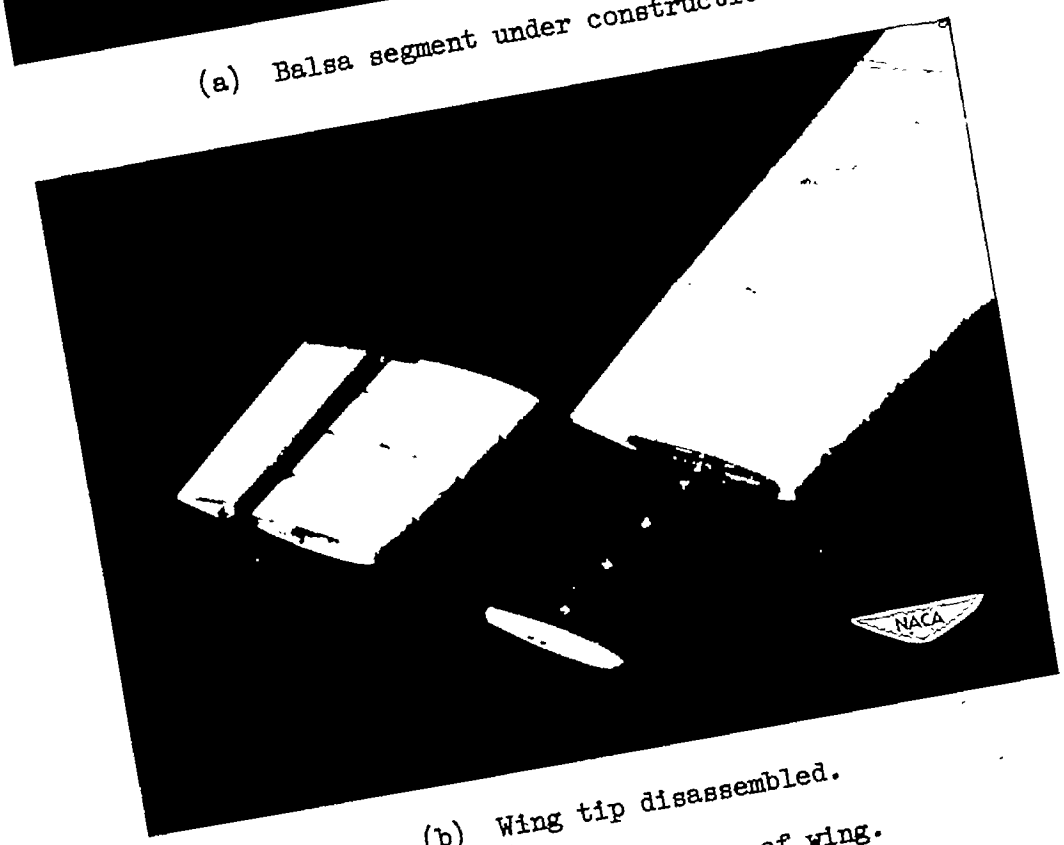

(b) Wing tip disassembled.

Figure 8.- Construction of wing.

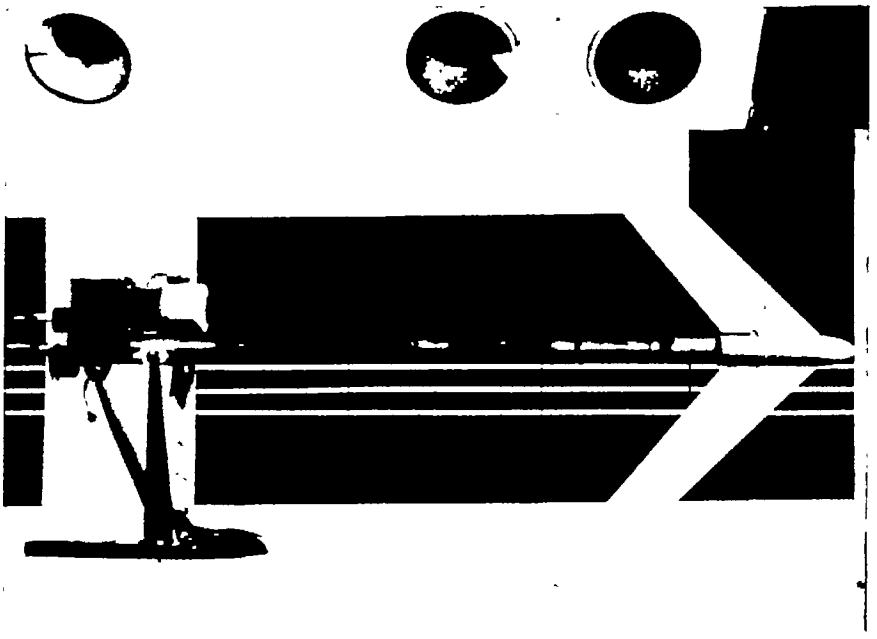

(a) Mounted in wind tunnel.

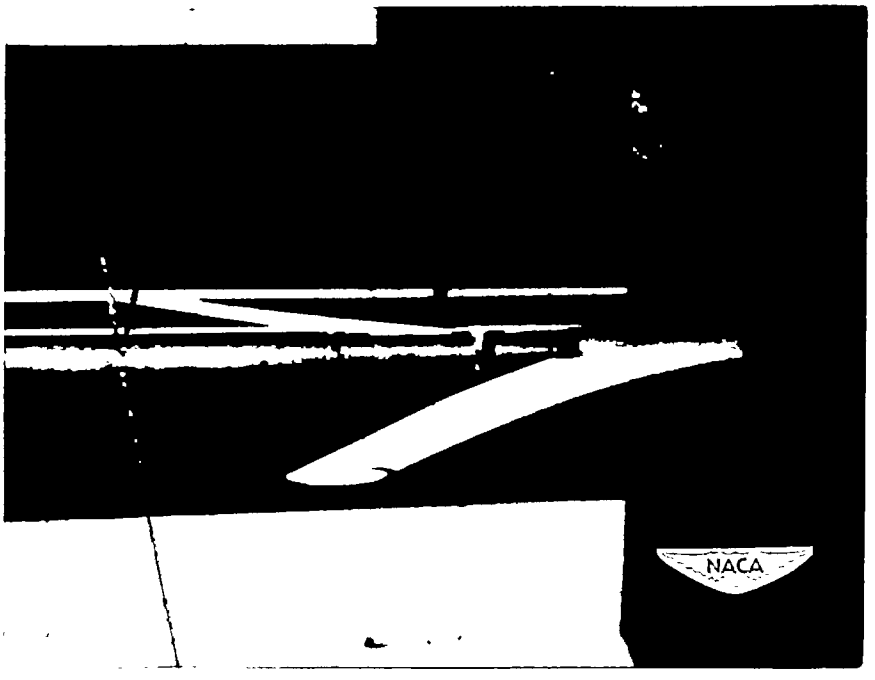

(b) Fixed in wind tunnel. 80-percent-span ailerons deflected 10°; $q = 30$.

Figure 9.- Photograph of swept wing.

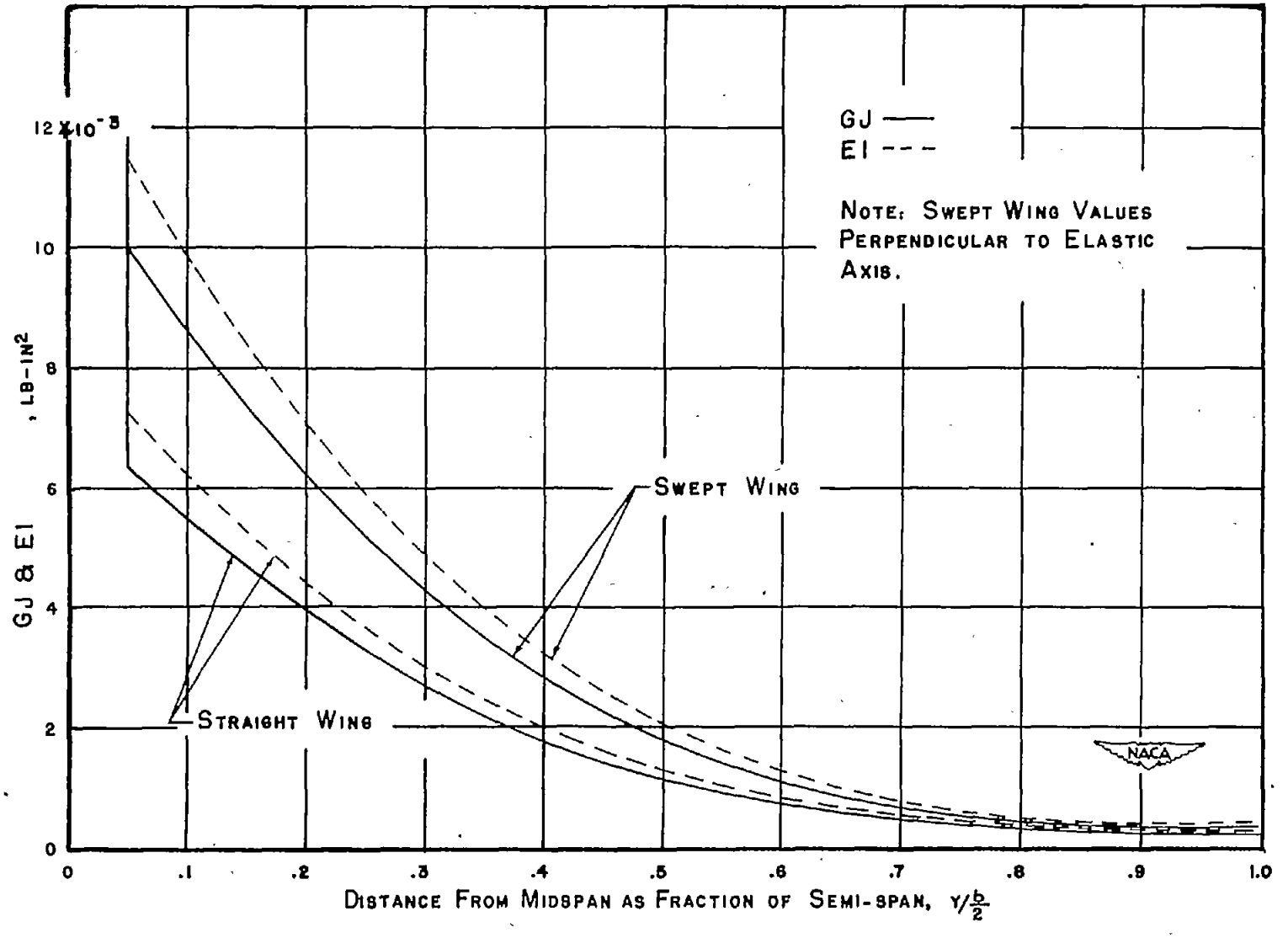

Figure 10.- Stiffness-distribution curves for straight and swept wings.

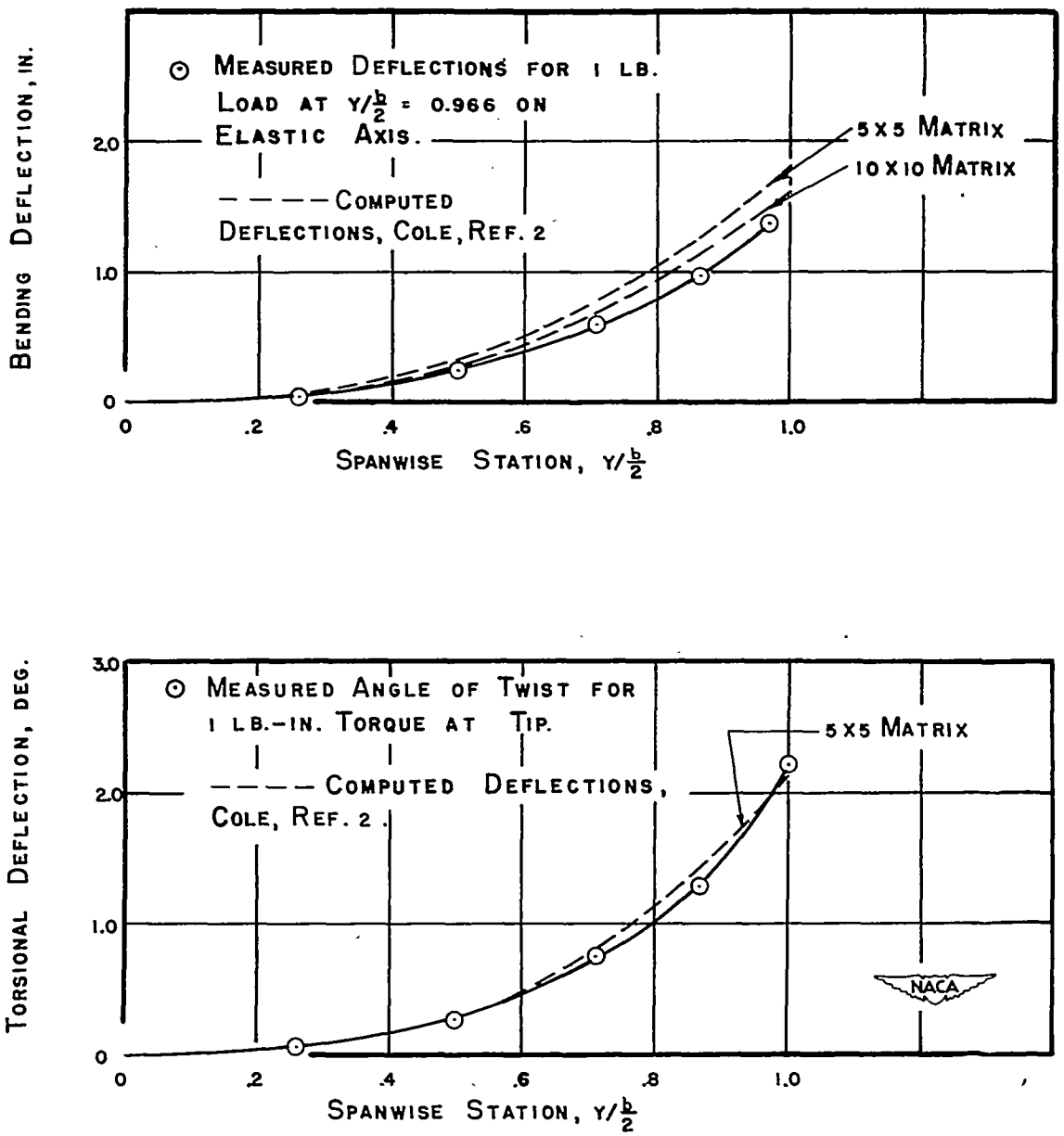

Figure 11.- Static deflections of straight wing.

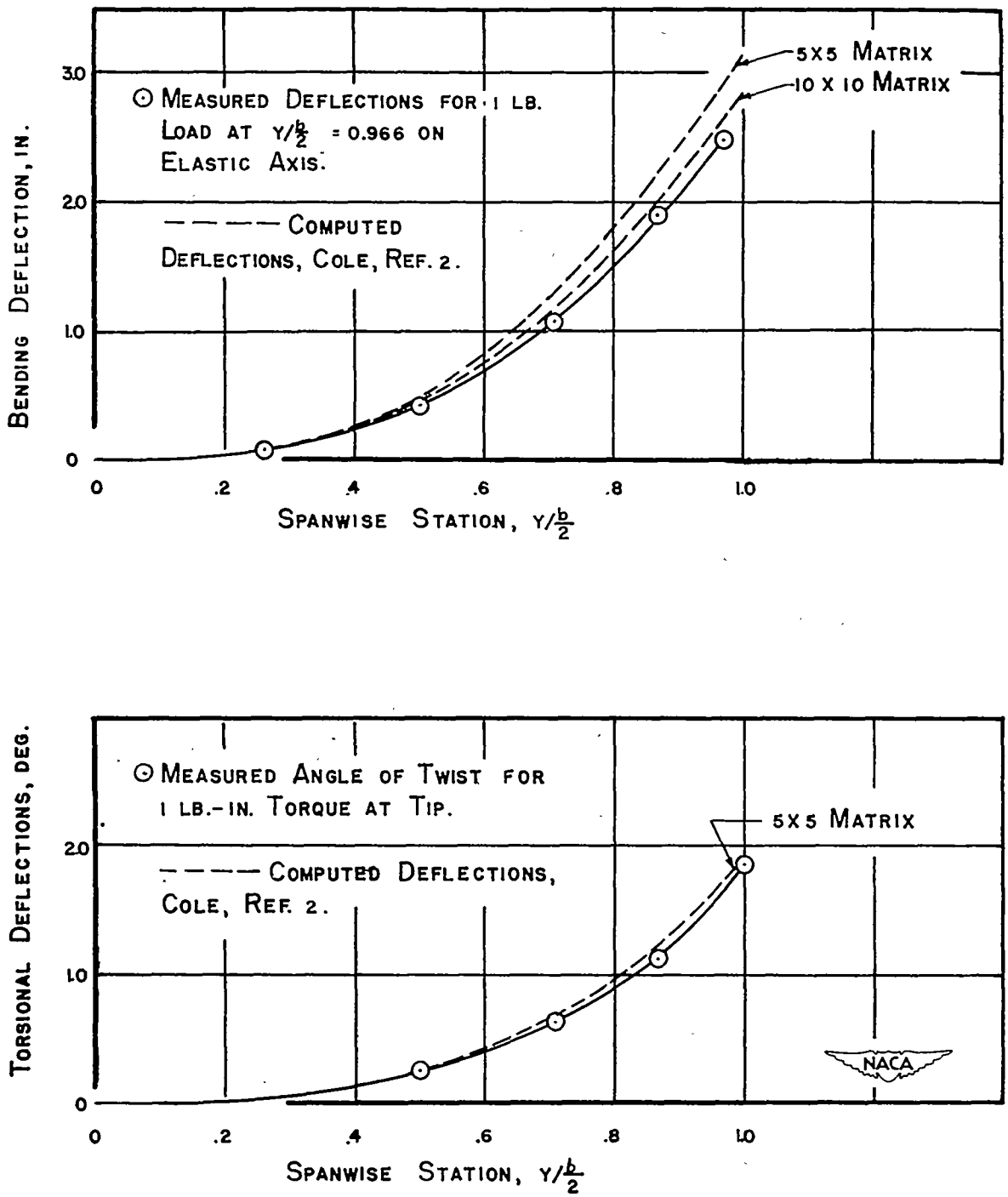

Figure 12.- Static deflections of swept wing.

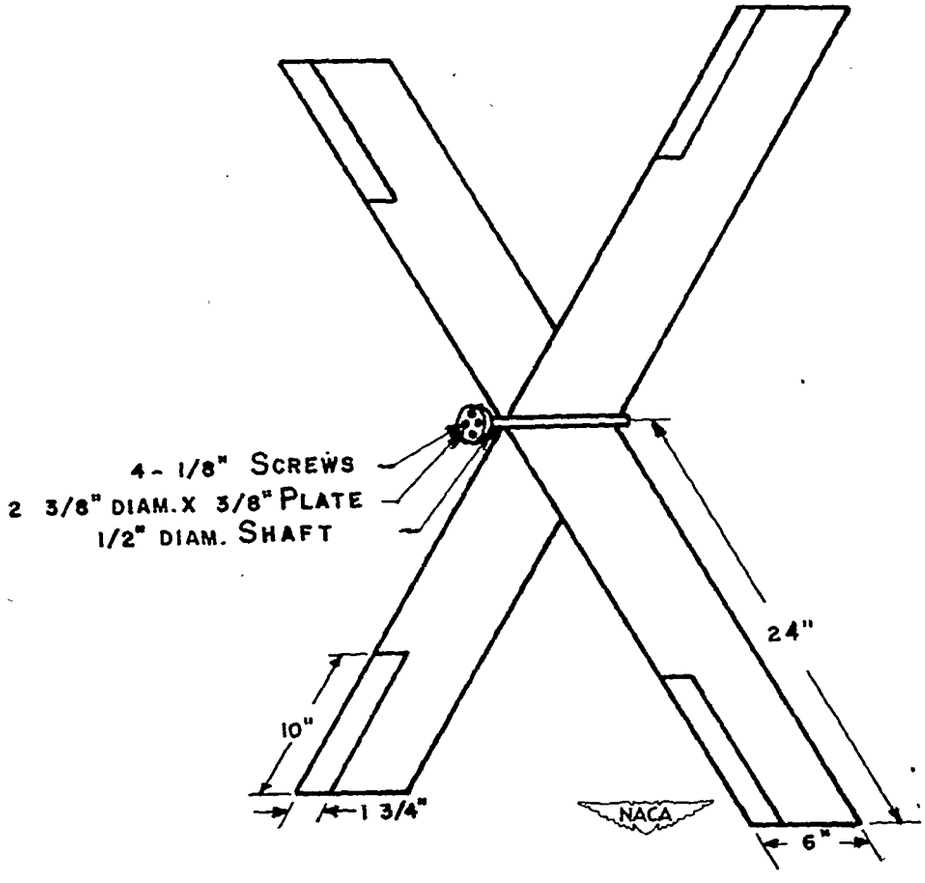

Figure 13.- Sketch of four-panel wing. Panels mounted mutually perpendicular.

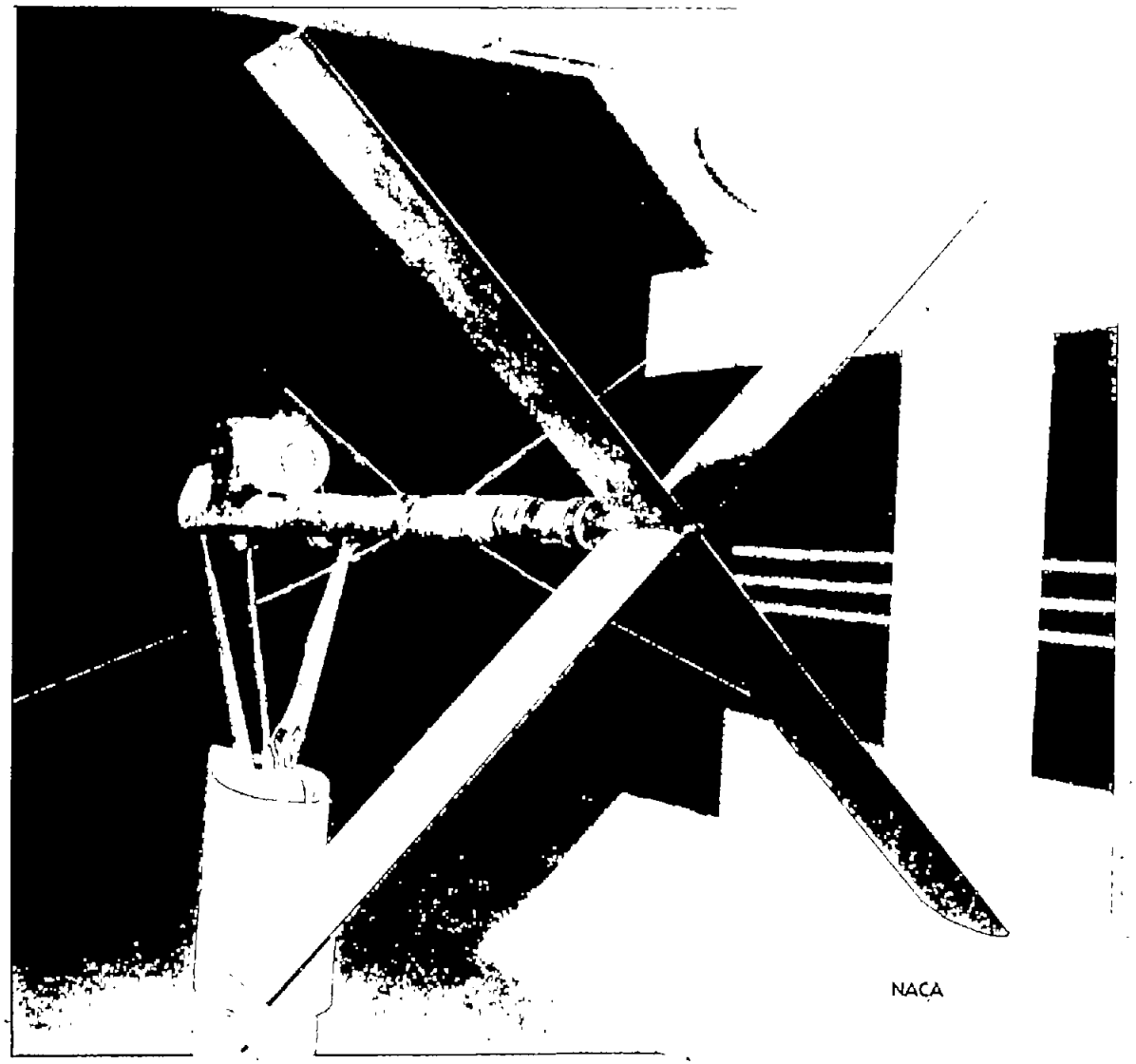

Figure 14.- Photograph of four-panel wing mounted in wind tunnel.

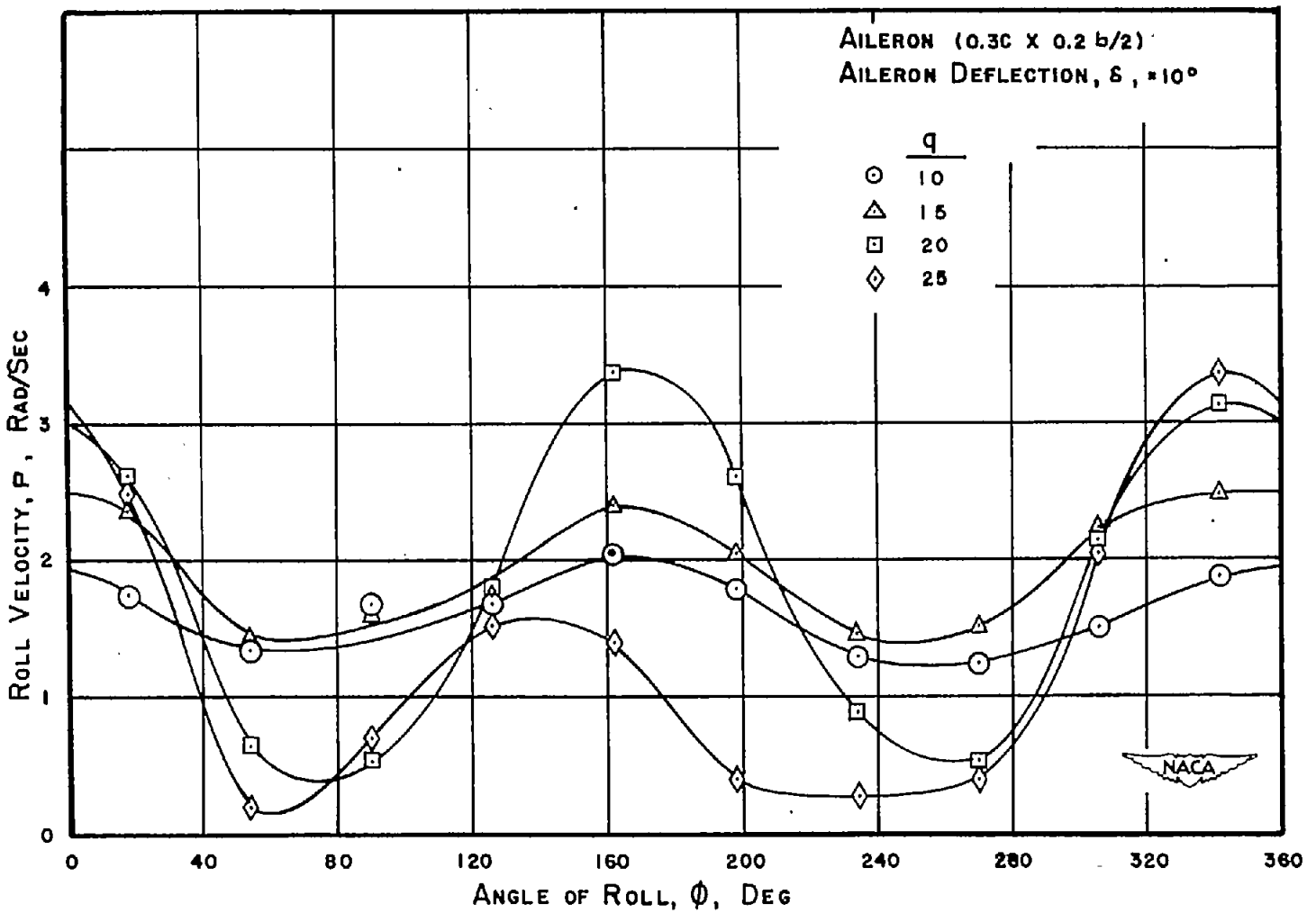

Figure 15.- Variation of roll velocity with angle of roll. Straight wing.

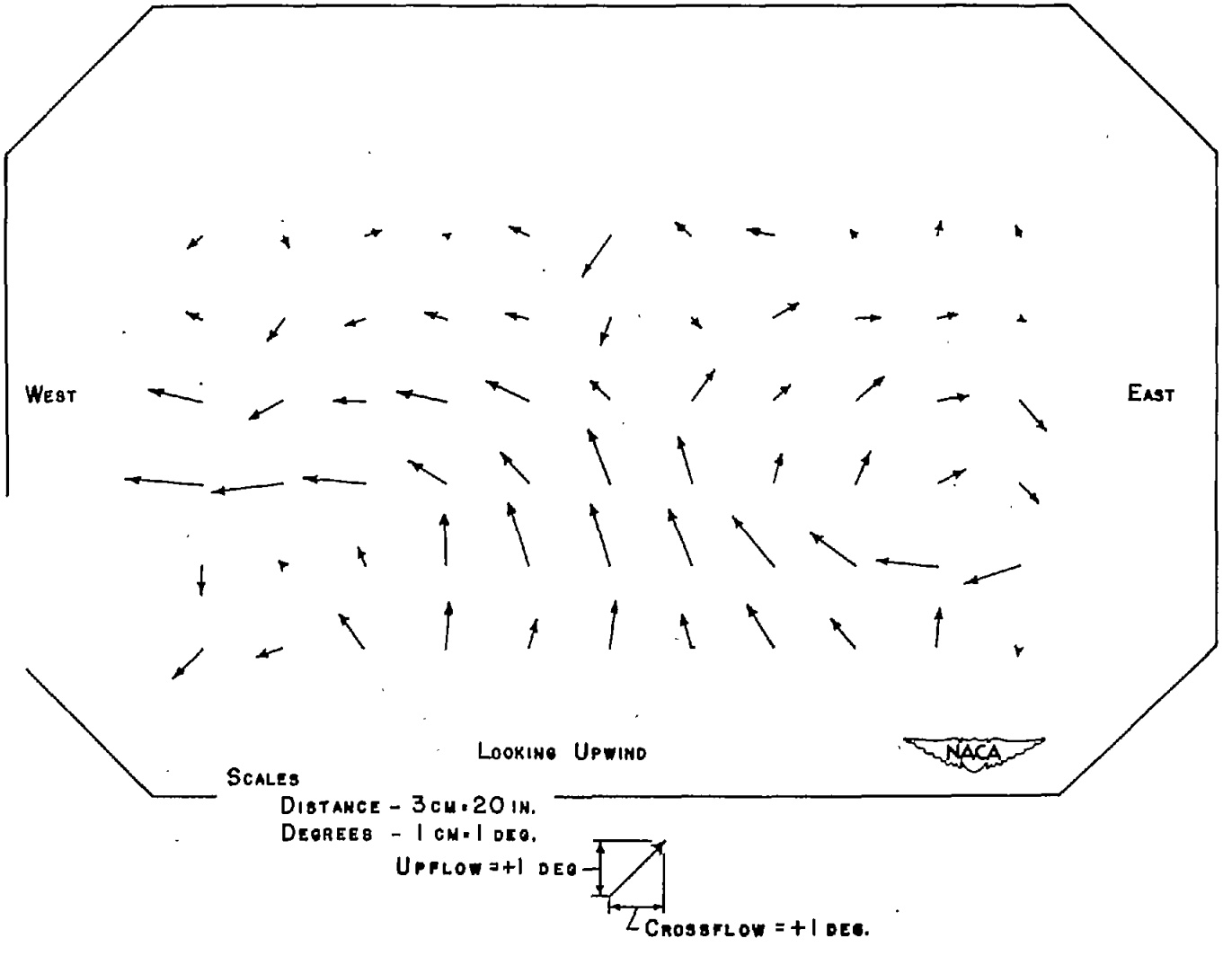

Figure 16.- Secondary-flow pattern at entrance of wind-tunnel test chamber.

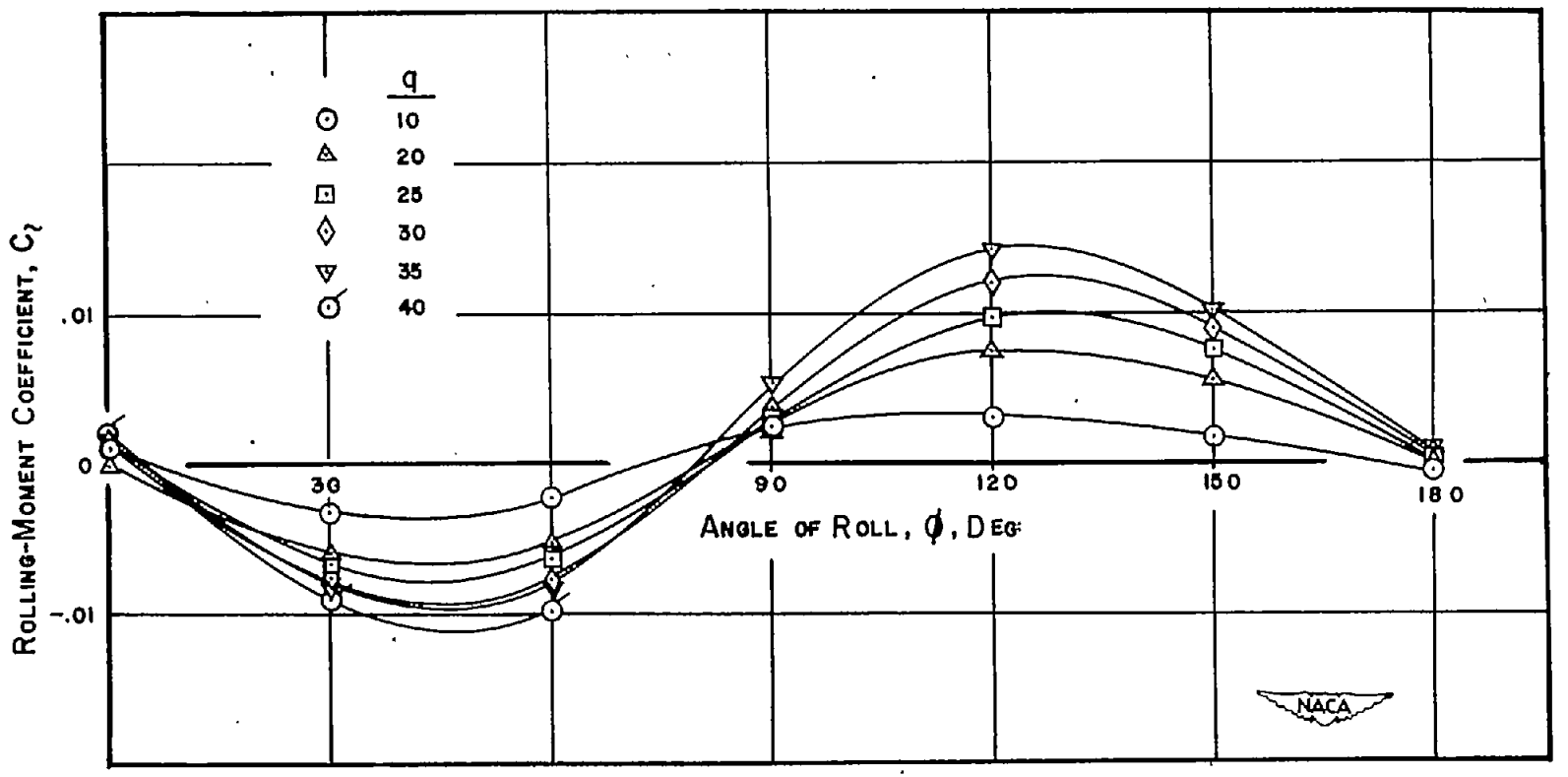

Figure 17.- Rolling-moment coefficient due to secondary flow in wind tunnel. Straight wing fixed at various angles of roll.

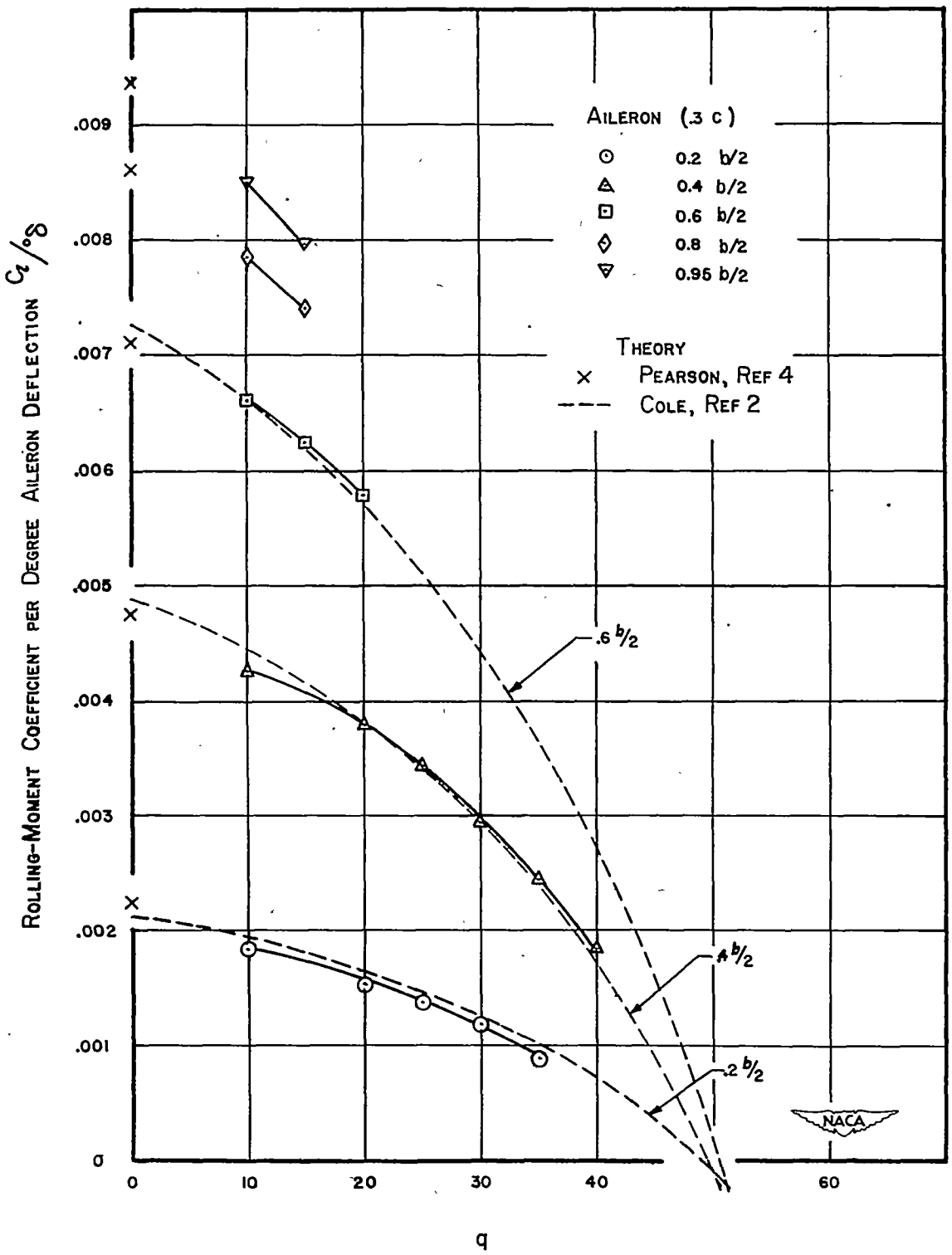

Figure 18.- Variation of rolling-moment coefficient due to aileron deflection with q. Straight wing.

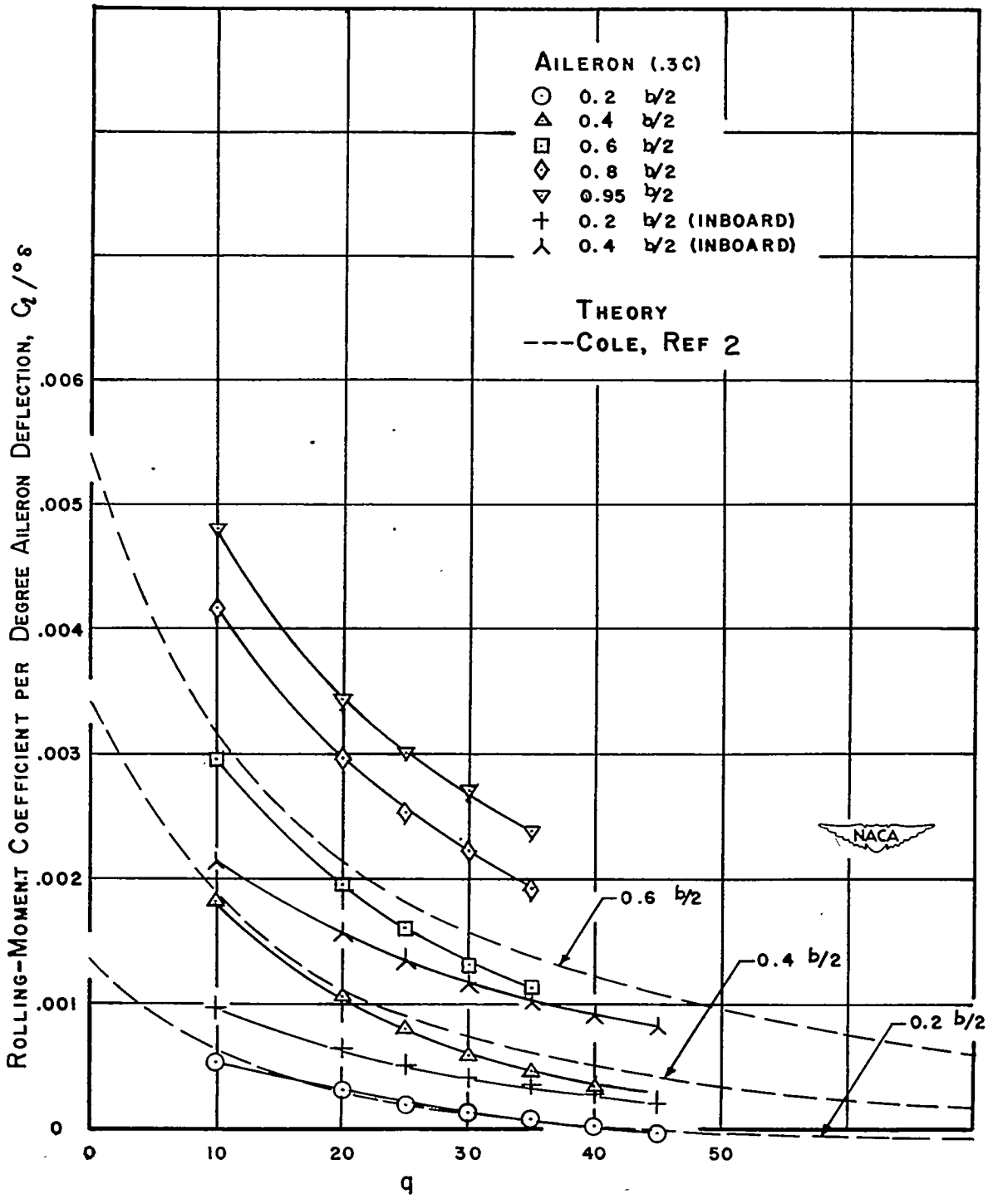

Figure 19.- Variation of rolling-moment coefficient due to aileron deflection with q. Swept wing.

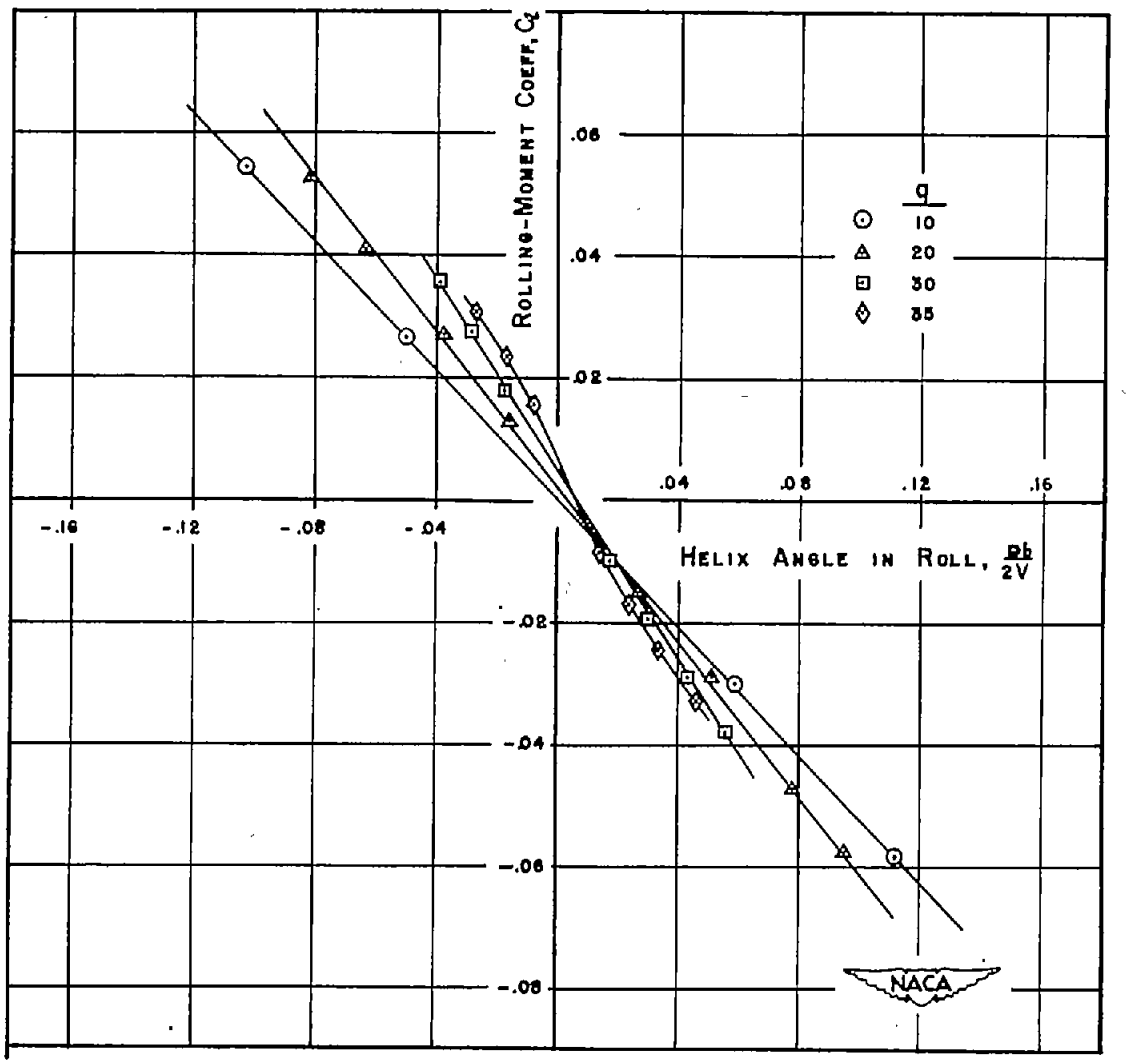

Figure 20.- Variation of damping-moment coefficient in roll with helix angle. Straight wing.

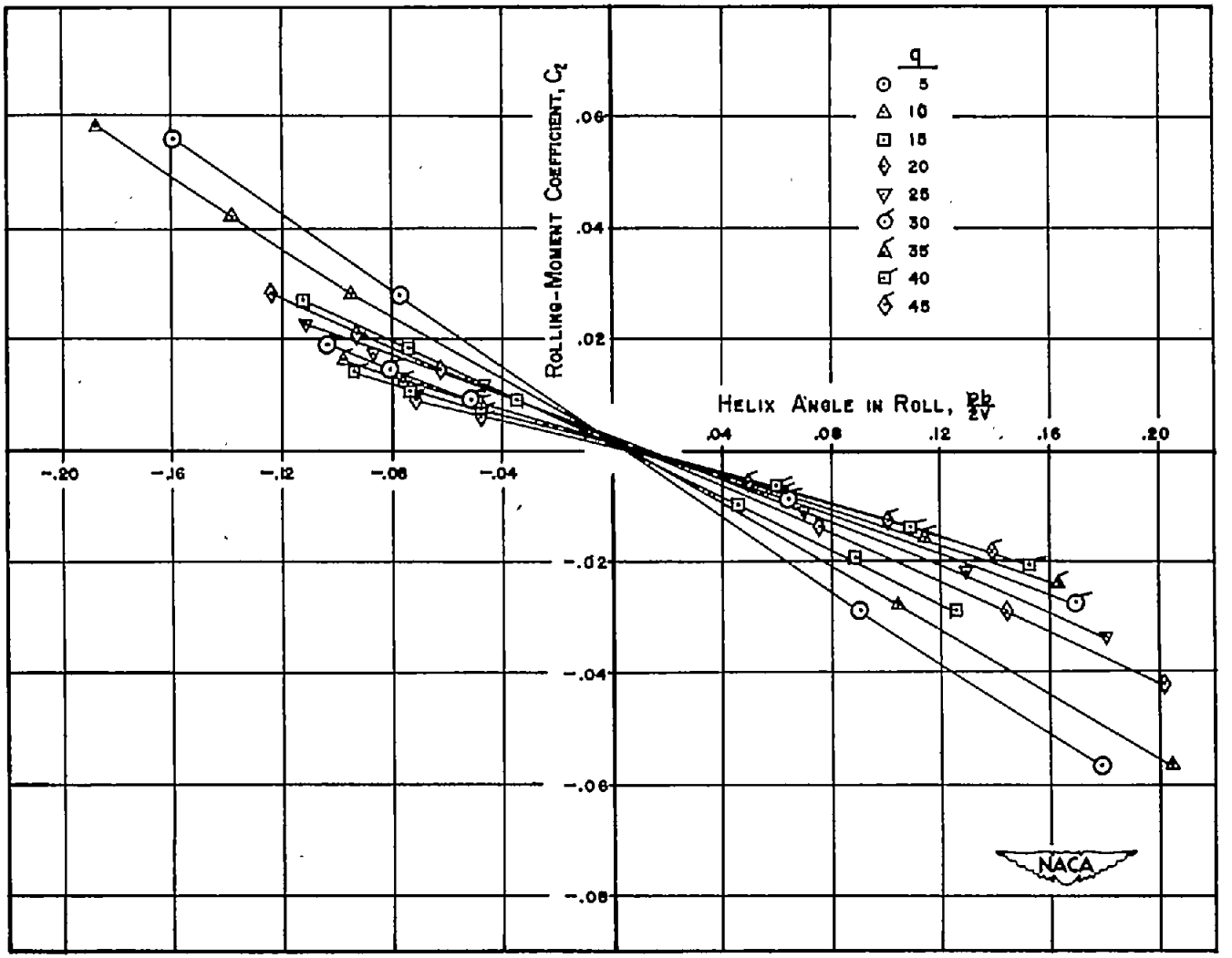

Figure 21.- Variation of damping-moment coefficient in roll with helix angle. Swept wing.

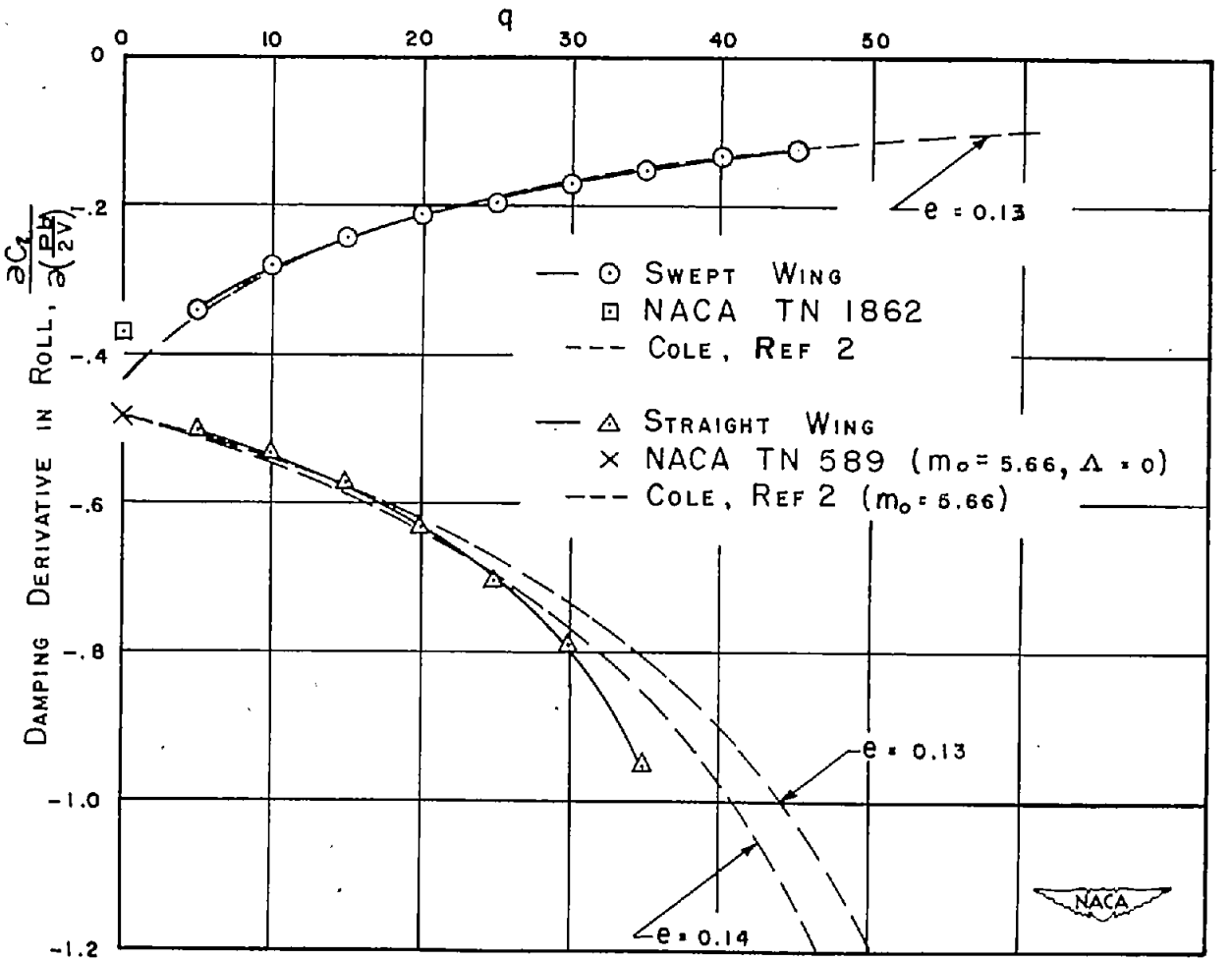

Figure 22.- Variation of damping derivative in roll with q. Straight and swept wings.

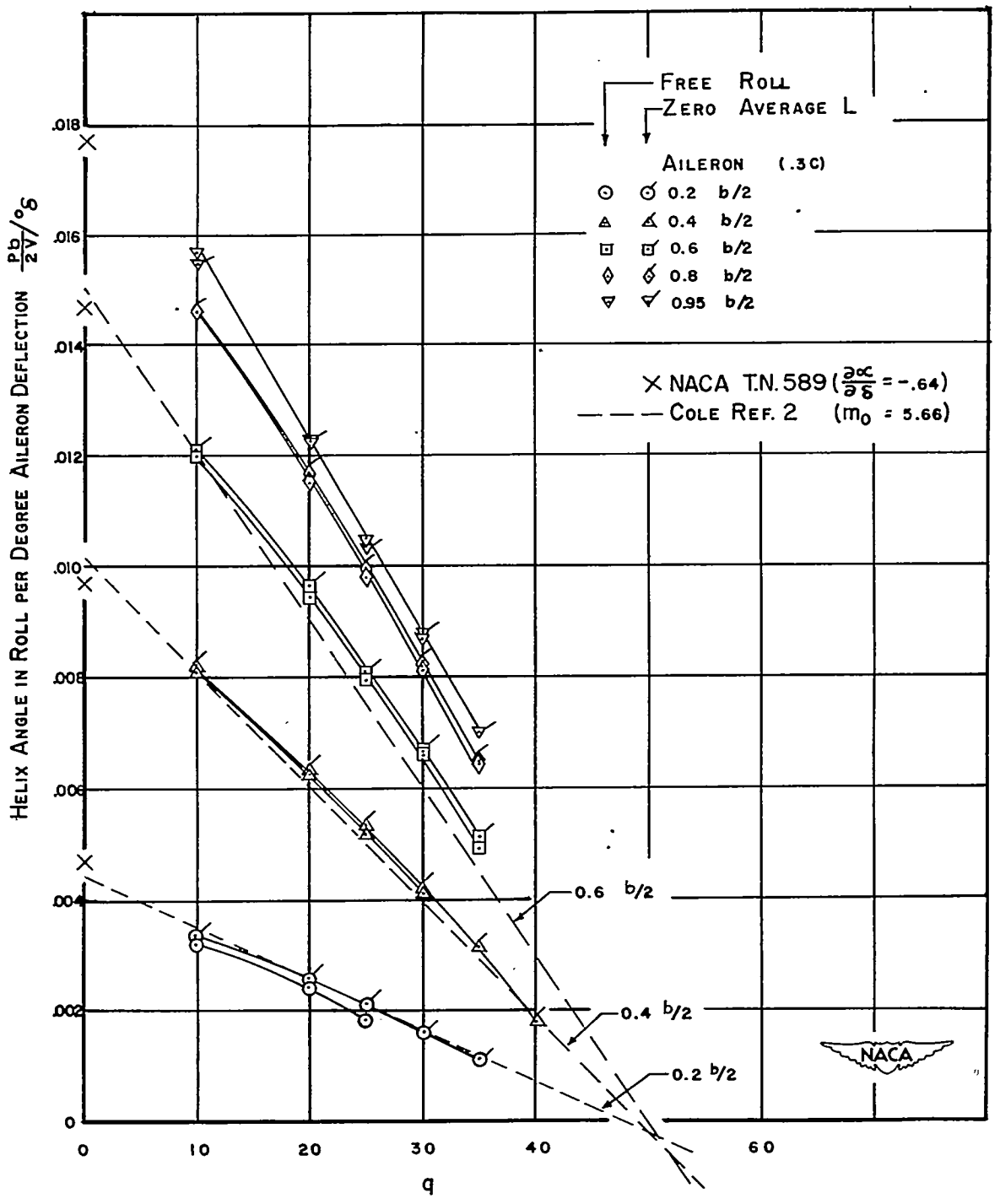

Figure 23.- Variation of helix angle in roll due to aileron deflection with q. Straight wing.

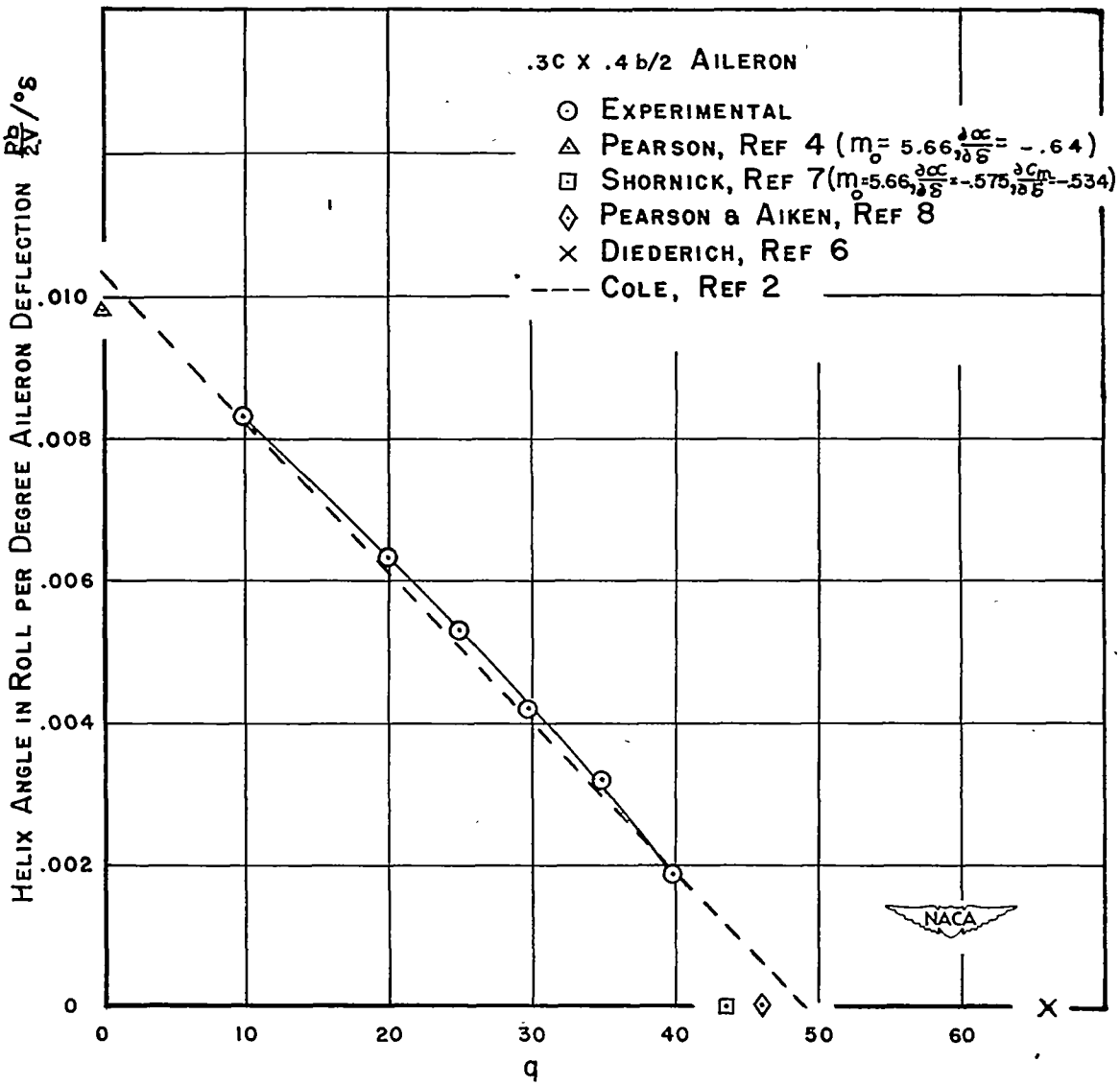

Figure 24.- Comparison of experimental and theoretical helix angle in roll. Straight wing with 0.3c × 0.4b/2 aileron.

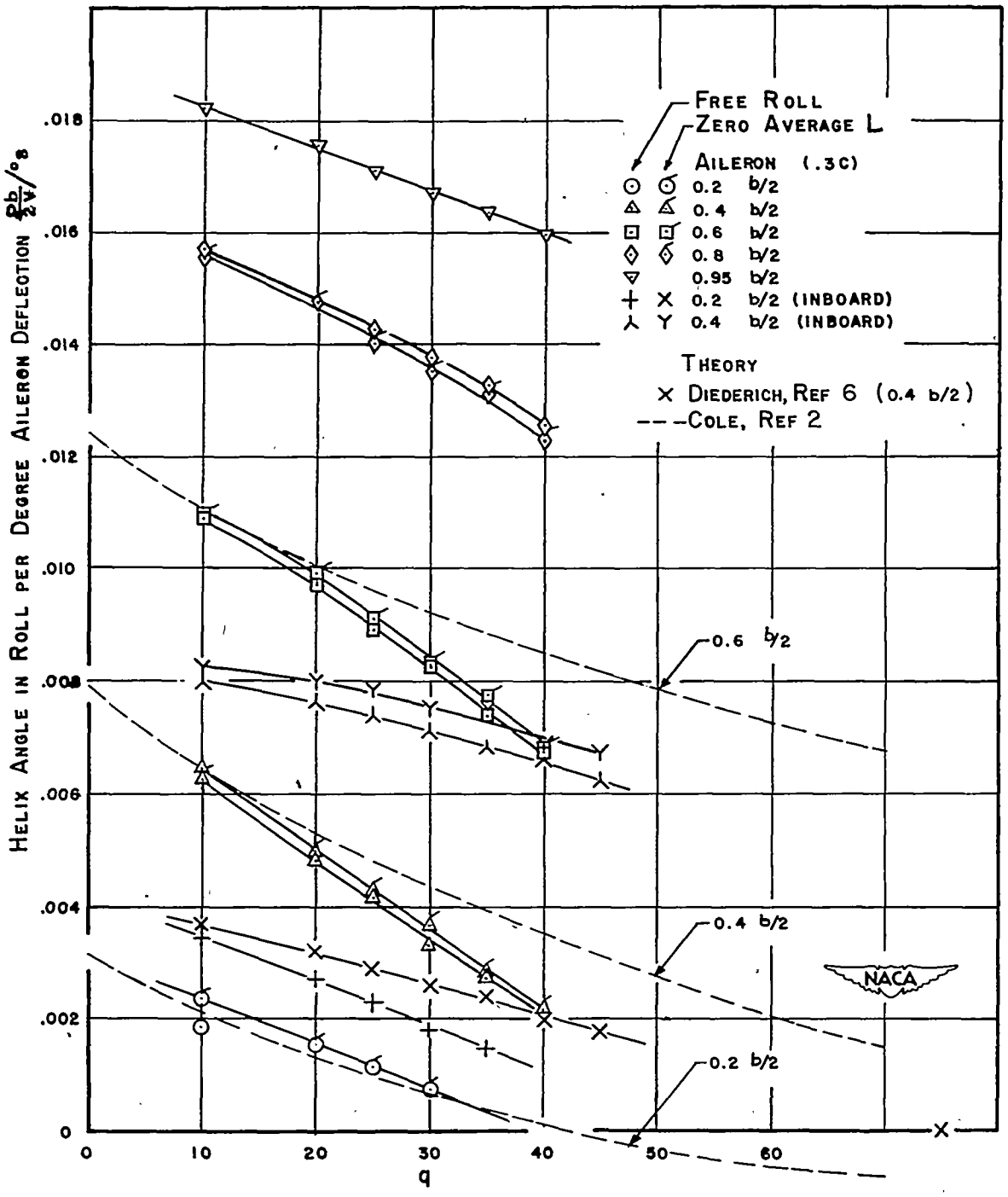

Figure 25.- Variation of helix angle in roll due to aileron deflection with q. Swept wing.

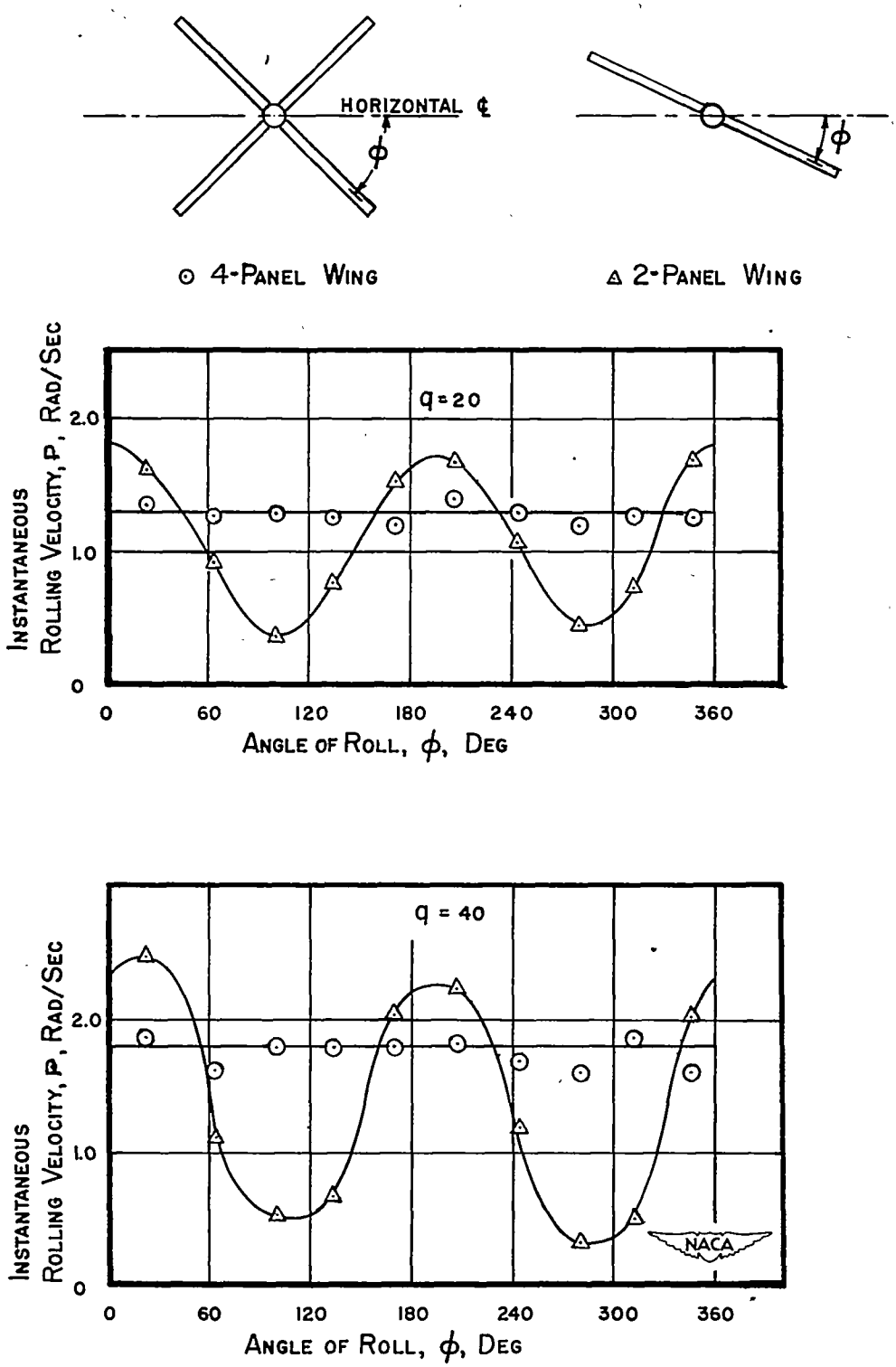

Figure 26.- Variation of instantaneous free-rolling velocity with angular position of model in tunnel. Two- and four-panel rigid straight wing.

NACA-Langley - 12-13-51 - 1000